universität wien

MASTERARBEIT / MASTER'S THESIS

Titel der Masterarbeit / Title of the Master's Thesis

„Trial-to-trial similarity and distinctness of muscle synergy activation coefficients increases during learning and with a higher level of movement proficiency“

verfasst von / submitted by

Paul Kaufmann, BSc

angestrebter akademischer Grad / in partial fulfilment of the requirements for the degree of

Master of Science (MSc)

Wien, 2023 / Vienna 2023

Studienkennzahl lt. Studienblatt / degree programme code as it appears on the student record sheet:	A 066 826
Studienrichtung lt. Studienblatt / degree programme as it appears on the student record sheet:	Masterstudium Sportwissenschaft
Betreut von / Supervisor:	Ass.-Prof. Mag. Hans Kainz, MSc PhD

Abstract

Muscle synergy analyses are used to increase our understanding of motor control. Spatially fixed synergy vectors coordinate multiple co-active muscles through activation commands, known as activation coefficients. To better understand motor learning, it is crucial to know how synergy recruitment varies during a learning task and different levels of movement proficiency. Within one session participants walked on a line, a beam, and learned to walk on a tightrope – tasks that represent different levels of proficiency. Muscle synergies were extracted over all conditions and the number of synergies was determined through the knee-point of the total variance accounted for (tVAF) curve. We found that the tVAF of one synergy decreased with task proficiency (line < beam < tightrope). Additionally, trial-to-trial similarity and distinctness of synergy activation coefficients increased with proficiency and after a learning process. We conclude that precise adjustment and refinement of synergy activation coefficients play a crucial role in motor learning.

Zusammenfassung

Muskel-Synergie-Analysen werden eingesetzt, um unser Verständnis der motorischen Kontrolle zu verbessern. Definierte Synergievektoren koordinieren mehrere gleichzeitig aktive Muskeln durch Aktivierungskoeffizienten. Um motorisches Lernen besser zu verstehen, ist es entscheidend zu wissen, wie sich die Aktivierung von Synergien während einer Lernaufgabe und bei unterschiedlichen Bewegungsfertigkeiten verändert. Teilnehmende Personen dieser Studie gingen innerhalb einer Datenaufnahme über eine Linie, einen Balken und lernten auf einem Seil zu gehen. Diese Aufgaben repräsentieren verschiedene Fertigkeitsniveaus. Muskel-Synergien wurden über alle Aufgaben berechnet und die Anzahl der Synergien wurde durch den Kniepunkt der Gesamtvarianz (tVAF) Kurve bestimmt. Die tVAF bei einer Synergie nahm mit zunehmender Aufgabenfertigkeit ab (Linie < Balken < Seil). Darüber hinaus nahmen die Variabilität und Unterscheidbarkeit der Aktivierungskoeffizienten von Synergien nach einem Lernprozess und mit zunehmender Aufgabenfertigkeit zu. Daraus lässt sich schließen, dass eine präzise Anpassung und Verfeinerung der Aktivierungskoeffizienten von Synergien eine entscheidende Rolle im motorischen Lernen spielen.

TABLE OF CONTENTS

Acknowledgements

My sincere appreciation goes to:

Reinhard Filzmoser, whose passion for sports inspired me to study sport science.

My family for their support and belief in me, allowing me to pursue my own path.

Sandra Walter, for her constant motivation and support throughout the research process.

All the participants whose vital contributions made this study possible.

The Neuromechanics research group for their invaluable assistance and guidance.

Hans Kainz for igniting my research passion and motivating me to enhance this work.

1 Introduction

The underlying mechanisms, by which the central nervous system controls movements and adapts during learning new movements, are still not fully understood. One common theory in in the field of motor control implies the idea of muscle synergies (Bizzi & Cheung, 2013; Bizzi et al., 1999; d'Avella & Bizzi, 2005). Put simply, muscle synergies refer to groups of co-active muscles, termed synergy vectors or motor modules, which are recruited by activation coefficients, corresponding to time-dependent control inputs of the central nervous system (Bizzi & Cheung, 2013; Bizzi et al., 1999). In line with Bernstein's levels of movement construction (Bernstein, 1967; Profeta & Turvey, 2018), this simplifies the complex coordination of the large number of muscles in the human body by controlling the activation of a limited number of spatially fixed, and temporally independent motor modules, rather than individually controlling each muscle.

Over the last two decades, muscle synergies, extracted from electromyography (EMG) recordings have been studied in healthy and pathological populations across various tasks. These studies have demonstrated the recruitment of similar motor modules in different movements, strengthening the concept of spatially fixed synergy vectors. So-called shared synergies describe similar movement fragments, which correspond to physical subtasks with the same mechanical goals (Nazifi et al., 2017). For example, shared synergies were found between walking and cycling (Barroso et al., 2014), walking and slipping (Nazifi et al., 2017), walking and standing reactive balance tasks (Allen et al., 2020), stepping and non-stepping postural behaviors (Chvatal et al., 2011), seated and standing cycling (Hug et al., 2011; Turpin et al., 2017) or overground and treadmill running (Oliveira et al., 2016). To describe the complexity of motor control, the total variance in muscle activity accounted for (tVAF) by a given number of synergies, and the number of needed synergies (NoS) are widely utilized parameters. For instance, less synergies and higher tVAF – indicating lower motor complexity – were found in individuals with cerebral palsy (Shuman et al., 2017; Steele, Rozumalski, et al., 2015) or stroke (Clark et al., 2010; Van Criekinge et al., 2020) compared to unimpaired populations, and in younger compared to older adults during walking (da Silva Costa et al., 2020).

It is generally accepted, that generating identical movements on successive attempts is impossible, due to an inherently noisy nervous system (Faisal et al., 2008). This noise can arise from either the central nervous system through movement planning or peripherical

structures (i.e.: force production by muscles). In 2017, Dhawale et al. reviewed recent studies regarding movement variability in motor learning, and concluded, that variability in the planning space is more likely a feature of motor system plasticity that drives motor learning, rather than unwanted noise. Moreover, this trial-to-trial variability decreases with increasing task proficiency (Cardis et al., 2018; Dhawale et al., 2017; Levy-Tzedek, 2017; Wu et al., 2014), aligning with the principles of reinforcement learning (Dhawale et al., 2017). Reinforcement learning theory suggests that a system learns new behaviors through trial-and-error (Kaelbling et al., 1996). Motor commands that lead to favorable outcomes (i.e.: successful execution of a movement task) are repeated, reinforced, and refined in subsequent attempts. In a study by Wu et al. (2014) participants were trained to replicate a curve shape using hand trajectories in a reaching task. They found that individuals who displayed higher kinematic variability prior to training showed faster rates of learning. Hence it seems that variability during the learning process increases the likelihood of finding the optimal motor command.

To date, only few studies have examined the role of muscle synergies in movement learning. For instance, Sylos-Labini et al. (2022) compared walking trial-to-trial variability of temporal synergy activations across different age groups, ranging from neonates to adults. They observed a decrease in variability during locomotor development. Consistent with a prior study on locomotor development (Dominici et al., 2011), authors revealed that motor complexity and the number of synergies increased with age. In adults, changes of activation coefficients variability correlated with changes in bowling scores across sessions (Cheung, Zheng, et al., 2020). Comparing professional ballet dancers with individuals without any dancing or gymnastics experience, Sawers et al. (2015) revealed higher trial-to-trial similarity with higher beam walking proficiency. Additionally, dancers showed lower variability within synergy vectors and higher spatial distinctness between synergy vectors. Similarly, dance-based rehabilitation in individuals with Parkinson's disease improved the consistency and distinctness of synergy vectors (Allen et al., 2017). All the mentioned studies were limited by either inter-participant variability (Hug, 2011; Pale et al., 2020; Scano et al., 2019; Sylos-Labini et al., 2022; Zhao et al., 2021), or inter-session variability (Hug, 2011; Kristiansen et al., 2016; Pale et al., 2020), which can be attributed to individual motor control differences and variations in skin-electrode impedance and electrode position.

To the best of our knowledge, no study has yet examined changes in muscle synergies using a within-participant, within-session protocol. Therefore, the present study addresses this

research gap. Briefly, each participant walked on a line, a beam, and a tightrope. The choice of these three tasks was based on the progression from an easy, daily task with highest movement proficiency (line) to a more uncommon task that was still manageable for participants (beam) and finally to a new task, which could be learned within one data collection session (tightrope). The twofold aim of the study was to examine if motor complexity, trial-to-trial similarity of activation coefficient and activation coefficient distinctness differs: (1) between an early and a late stage of a learning process (i.e.: learning to walk on a tightrope); (2) between common and less common movement tasks – addressing movement proficiency. Subsequently, we investigated, if the contribution of synergies changes among learning or proficiency changes. The study primarily focused on muscle synergies, but trial-to-trial similarity of EMG envelopes and joint angles were also analyzed to gain a comprehensive understanding of variability in motor learning. Additionally, the study investigated whether the amount of muscle activity changes after learning, building on previous findings by Donath et al. (2016), who showed decreased muscle activity after slackline training. We hypothesize that motor complexity, activation coefficient distinctness and trial-to-trial similarity of synergy activation, EMG envelopes, and joint angles (1) gets higher during learning, and (2) is higher in more common movements. Furthermore, the study hypothesizes that the amount of muscle activity decreases during learning (1) and is lower in more common movements (2).

2 Materials and Methods

2.1 Participants

This study involved ten healthy participants (age: 25.2 ± 3.34 years; bodyweight: 69.9 ± 7.34 kg; height: 1.76 ± 0.09 m; body-mass-index: 22.63 ± 1.51; 6 men and 4 women) without neurological or orthopedic impairments, who were not able to walk on a slackline or tightrope beforehand. The study was approved by the ethics committee of the University of Vienna (reference number: 00820) and participants gave written informed consent.

2.2 Experimental Setup and Data Collection

Each participant walked under different tasks: (a) a line taped on the ground (LINE; length: 310 cm; width: 1.4 cm); (b) a beam (BEAM; length: 341.5 cm; width: 10 cm; height: 28.5cm) and (c) a tightrope (TIGHTROPE; length: 363 cm; diameter: 0.9 cm; height: 363 cm) spanned between two platforms (Figure 1). The learning process for walking on the TIGHTROPE was divided into two stages: TRfail and TRsucc. TRfail included the first five attempts where participants were able to perform at least one full gait-cycle of the right leg but were not able to successfully balance over the entire TIGHTROPE. TRsucc included the attempts where participants successfully balanced over the TIGHTROPE in four out of five consecutive attempts. A successful attempt was defined as walking over the whole TIGHTROPE and maintaining balance on the second platform. If a participant was able to successfully balance over the TIGHTROPE in two out of the first five attempts, the difficulty of the task was increased with visual constraints, by either an eye-patch over the left eye, or further by closing both eyes (if two of the first five trials were successful with the eye-patch). The conditions were recorded in the following order: (1) LINE-walking (startLine), (2) BEAM-walking (startBEAM), (3) start of learning process on the TIGHTROPE (TRfail) until (4) the end of learning process (TRsucc), (5) BEAM-walking (endBEAM), and (6) Line-walking (endLINE). To ensure consistent visual constraints across tasks for later comparisons, five trials with opened eyes, an eye-patch over the left eye and both eyes closed were recorded each time (start and end) for LINE and BEAM. As data from the first right stance phase was further analyzed, we aimed to minimize transient accelerations at the onset step (da Silva Costa et al., 2020; Oliveira et al., 2014; Shuman et al., 2017), by instructing participants to start each trial with their left leg. Only the stance phase was analyzed, to neglect highly variable movement times between stance and swing phases across conditions (Ghislieri et al., 2023; Hug, 2011). No additional constraints for pause time, step cadence,

step length, or hints for walking over the TIGHTROPE were given, to provide self-directed learning.

Figure 1: *Top image shows the upside-down gymnastics bench which was used for BEAM conditions. Bottom image shows the THIGHTROPE mounted on a rack between two platforms.*

Prior to the data collection, thirteen surface EMG sensors (eleven PicoEMG and two Mini Wave Infinity, Wave Plus wireless EMG system, Cometa, Milan, Italy) were placed on the trunk and right limb following the Seniam guidelines (Seniam.org) and recommendations from previous studies (Huebner et al., 2015; Oshikawa et al., 2020; Vera-Garcia et al., 2009): tibialis anterior (tib_abt), peroneus longus (per_long), soleus, gastrocnemius medialis (gast_med), vastus lateralis (vast_lat), rectus femoris (rect_fem), biceps femoris (bic_fem), semitendinosus (sem_tend), gluteus maximus (glut_max), rectus abdominis (rect_abd), extensor obliques (ext_obli), multifidus (multifid) and erector spinae iliocostalis (erec_spin). A baseline EMG signal of several seconds was collected (EMG_base) while participants lied in a supine and relaxed position on a massage table. The standard Vicon Plug-in-Gait marker set (Vicon, Oxford, UK), including 21 reflective markers, were placed on the legs and the trunk of each participant (Kadaba et al., 1990). The heel and toe markers were placed on the shoes of participants, similar to Paterson et al. (2017). A 12-camera 3D motion capture system (Vicon, Oxford, UK) was used to record marker trajectories with a sampling rate of 200 Hz, EMG data with 1000 Hz and ground reaction forces of one force plate with 1000 Hz (Kistler Instrumente, Winterthur, Switzerland), simultaneously. In addition, participants wore in-shoe force sensor soles (loadsol®, Novel, Munich, Germany), which were used to determine stance phases. Insoles data was captured with 200 Hz (loadsol-s android application version 1.7.63) on a mobile phone (Huawei P30 Lite, Huawei, Shenzhen, China) and brought to zero level every 5 to 10 trials to minimize errors due to sensor drifts. Foot contact instances were determined by vertical contact forces over 30 Newton via custom scripts. Time synchronization between the Insole and Vicon data was achieved by participants stepping on a force plate at the beginning of each trial. The experimental data

was captured and processed using Vicon Nexus 2.12 software (Vicon, Oxford, UK). Subsequent analyses were conducted using Gnu Octave version 6.2.0 (Eaton et al., 2021) and MATLAB (R2022a, Mathworks Inc., Natick, USA).

2.3 EMG processing

Raw EMG signals were high-pass filtered at 25 Hz (4^{th}-order Butterworth zero lag filter) to remove movement artefacts (Hug et al., 2012; Potvin & Brown, 2004; Shuman et al., 2017; van der Krogt et al., 2016), demeaned, full-wave rectified and low-pass filtered at 7 Hz (4^{th}-order Butterworth zero lag filter), similar to previous gait studies (Ballarini et al., 2021; Boccia et al., 2018; Kim et al., 2016; Rabbi et al., 2020; van den Hoorn et al., 2015). The low-pass cutoff frequency of 7 Hz was chosen as a compromise between the different movement times (Figure 8). After filtering, baseline noise was removed by subtracting the root-mean-square of the filtered EMG_base signal, to improve signal-to-noise ratio (Frey Law et al., 2010; Hiep Vu Nguyen et al., 2016; Roh et al., 2013; Turpin et al., 2021), and resulted negative values were set to zero. Based on a visual inspection of raw and filtered EMG envelopes, trials with artefacts were removed, resulting in four to five remaining trials per condition. Afterwards signals were time-normalized to 101 data points (100% of stance phase) and amplitude normalized to values between 0 and 1, where an amplitude of 1 was equal to the maximum activation amplitude of a muscle among all trials (Bianco et al., 2018; Clark et al., 2010; Ghislieri et al., 2023; Kim et al., 2016; Oliveira et al., 2014).

2.4 Synergy extraction and determining the number of synergies

For each participant, processed EMG signals of trials from all conditions were concatenated (Hagio et al., 2015; Hug et al., 2011) and muscle synergies were extracted according to the spatial/synchronous synergy model. According to this model, motor control of muscle activations (EMG signals), is described by a linear combination of a fixed spatial synergy vector and a time-varying activation coefficient (Ghislieri et al., 2023; Profeta & Turvey, 2018; Turpin et al., 2021). Non-negative-matrix-factorization (NNMF) has been shown to be the most appropriate method for extracting muscle synergies in walking (Rabbi et al., 2020). Therefore, we used the "nmf_bpas" octave function (Kim & Park, 2008), an advanced algorithm of the classic NNMF (Lee & Seung, 2001; Paatero & Tapper, 1994; Seung & Lee, 1999) to extract one to twelve (number of muscles -1) muscle synergies. Instead of random inputs, the NNMF was initialized with outputs of the nonnegative single-value-decompensation with low-rank correction algorithm (Atif et al., 2019) to improve NNMF

(Atif et al., 2019; Boutsidis & Gallopoulos, 2008; Soomro et al., 2018; Turpin et al., 2021). Extracted synergy vectors were normalized to 1 based on their maximum values, and activation coefficients were multiplied by the same normalization values, to keep their product constant (Banks et al., 2017; Safavynia & Ting, 2012). More information regarding the synergy extracting procedure is provided in the supplementary material.

The total variance accounted for (tVAF) was calculated for each number of extracted synergies (1 to 12). It quantifies the reconstruction accuracy after the factorization, and is defined as the uncentered Pearson's correlation in percentage (Ballarini et al., 2021). To determine the number of synergies that represents motor control across all conditions (NoS), knee point analysis was employed (Ballarini et al., 2021; Ghislieri et al., 2023; Hug et al., 2012; Tresch et al., 2006; Turpin et al., 2021). The knee-point (v) was defined as the point on the tVAF curve that exhibits the smallest angle among three adjacent points (v-1, v, v+1). This approach assumes that beyond the knee-point, only unstructured data or noise is explained by additional motor modules (Tresch et al., 2006). It was preferred over threshold-based methods, as it has been shown to perform better (Ballarini et al., 2021) and is not affected by different low-pass filter cutoff frequencies (Hug et al., 2012). We further constrained our analysis by exclusively determining the knee-point for synergies with a tVAF exceeding 95%. This widely used threshold (Ballarini et al., 2021; Hagio et al., 2015; Hiep Vu Nguyen et al., 2016; Meyer et al., 2016; Rodriguez et al., 2013; Steele, Tresch, et al., 2015; van den Hoorn et al., 2015) was added based on visually observing sharp jumps in some tVAF curves, likely caused by the split of a synergy due to salient features (Ting & Chvatal, 2010).

2.5 Assessment of trial-to-trial similarity

The trial-to-trial similarity of synergy activation coefficients, EMG envelopes and joint angles were all quantified based on the same three parameters: the Pearson correlation coefficient (r), the maximum value of the normalized cross-correlation coefficient (r_{max}) and the lag time (lag% in % of the stance phase) where r_{max} occurred which represents the time shift between two curves. These parameters are widely used to quantify variabilities in synergy, EMG and kinematic waveforms (Banks et al., 2017; Barroso et al., 2014; Frère & Hug, 2012; Hug et al., 2011; Ivanenko et al., 2004; Ogihara et al., 2020; Turpin et al., 2017). We calculated them for every pairwise combination of trials in each condition within each synergy, muscle, and joint. The averaged value per condition represents the overall trial-to-trial similarity for synergy activation coefficients, EMG envelopes and joint angles.

2.6 Synergy analyses

We computed the tVAF using the EMG signals, synergy vectors and activation coefficients of each condition. Then, tVAF of one synergy (tVAF1) and tVAF at NoS (tVAFNoS) were compared across conditions to evaluate movement complexity (tVAF1) and the goodness of reconstruction (tVAFNoS). The distinctness of activation coefficients was determined by calculating the average value of all pairwise combinations of activation coefficients from different synergies within each trial for each condition. High values of r and r_{max}, along with small time-shifts (lag%), indicate a similarity in timing and a substantial amount of overlapping in synergy activations (Clark et al., 2010; Soomro et al., 2018).

Additional to the overall trial-to-trial similarity of each condition, we aimed to reveal, if differences in the variability just occur in some synergies. To classify similar synergy vectors among participants, we used k-means clustering (kmeans function in Octave – see appendix) similar to recent synergy studies (Cheung, Zheng, et al., 2020; Kim et al., 2016, 2018; Scano et al., 2019; Sylos-Labini et al., 2022). We computed the k-means clustering solution for a range of two to twelve clusters and repeated the process 100 times. For each repetition and each number of clusters, we calculated the average silhouette value (Rousseeuw, 1987). The optimal number of clusters was then determined on the point at which the maximum silhouette values plateaued – indicating small within- and high between-cluster distances (Cheung, Zheng, et al., 2020) (Figure 4). Trial-to-trial similarity parameters (r, r_{max}, lag%) were calculated for synergies within the same cluster, for each condition. For instance, if a cluster consisted of eight synergy vectors, the trial-to-trial similarity of that cluster was determined by averaging the trial-to-trial similarity values of the eight synergies. To examine the task-specific relevance of individual synergies, tVAF by each synergy was computed for every trial. These tVAF values were then averaged across synergies within the same cluster.

2.7 EMG analyses

To quantify changes in the amount of muscle activity, the root-mean-square (RMS) of the preprocessed EMG signals of every trial was calculated and averaged across trials of the same condition, within each muscle. Additionally, to the overall trial-to-trial similarity (section 2.5), correlation values were also averaged for each muscle to evaluate, if variability in activation patterns only occurred in some muscles (results provided in appendix).

2.8 Kinematic analyses

Joint angles were computed with OpenSim (Delp et al., 2007) using the recently introduced addBiomechanics.org application (Keenon et al., 2022). This application uses a bilevel optimization and enables to personalize musculoskeletal models and calculate joint angles in an easy and efficient way. We used the default option with the Rajagopal2015 model for human gait (Rajagopal et al., 2016). The computed joint angles were smoothened using a 6 Hz low-pass filter (4^{th}-order Butterworth zero lag filter) and time normalized to 101 datapoints of the stance phases. The following joint angles of the right leg and trunk were examined: ankle plantar-/dorsiflexion, knee flexion/extension, hip flexion/extension, hip ab-/adduction, hip internal/external rotation, lumbar flexion/extension, lumbar medial/lateral bending, and lumbar internal/external rotation. In addition to the overall trial-to-trial similarity (section 2.5), correlation values were also averaged for each joint separately, to evaluate, if variability in kinematics only occurred in some joints (results provided in appendix).

2.9 Statistics

We employed a two-way repeated measures ANOVA with TASK (LINE, BEAM, TIGHTROPE) and TIME as factors on all variables described above. The first time point (START) consisted of startLINE, startBEAM, and TRfail, while the second time point (END) included endLINE, endBEAM, and TRsucc. TASK was used to assess differences regarding task commonness – our second research question - including post hoc pairwise comparisons with Bonferroni correction. To address our first research question, i.e. changes during the learning process, – we calculated contrasts between TRfail and TRsucc. Furthermore, contrasts between startLINE and endLINE were examined as a baseline to assess the stability of the analyzed variable, as no differences were anticipated between the two LINE conditions. Additionally, contrasts between startBEAM and endBEAM were analyzed to explore potential transfer effects of learning from one balancing task (TIGHTROPE) to another (BEAM). Contrasts were conducted only if a significant difference was observed in any of the ANOVA outcomes (TASK, TIME, TASK*TIME). Prior, sphericity was checked with Mauchly-test (if necessary, Greenhouse-Geisser correction was applied), and normal distribution was verified with Shapiro Wilk-test. If the requirement of normal distribution was violated, an aligned-rank-transformation was performed. This transformation enabled us to conduct factorial ANOVA's on nonparametric

data (Elkin et al., 2021; Higgins et al., 1990; Wobbrock et al., 2011) and was utilized with ARTool 2.1.2 software (Washington, USA). Statistical analyses were performed with JASP 0.17.2 (Amsterdam, Netherlands). The alpha level was set at 0.05, and the results were reported at three levels of significance: $p < 0.05$, $p < 0.01$, and $p < 0.001$.

3 Results

Participants required 2.6 ± 1.4 attempts (range: 1 to 5) to perform their first complete gait-cycle with the right leg (TRfail) and 49.4 ± 22.8 attempts (range: 12 to 101) to complete the learning task (TRsucc). Two participants walked on the TIGHTROPE with visual constraints (1x eye-patch, 1x closed eyes).

3.1 Muscle synergy analyses

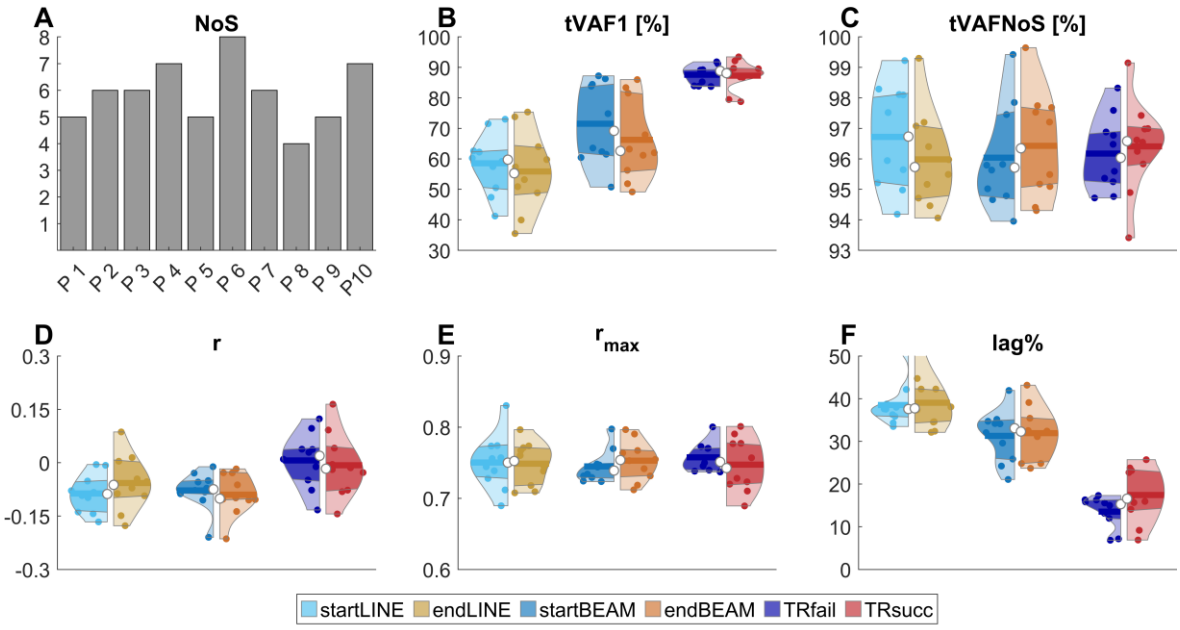

Figure 2: A: *bars show the number of required synergies (NoS) for each participant (P1 – P10).* ***B-C:*** *the total variance accounted for one synergy (**B:** tVAF1) and NoS (**C:** tVAFNoS).* ***D-F:*** *Synergy activation coefficient distinctness measured by Pearson correlation (**D:** r), maximum cross-correlation coefficient (**E:** r_{max}) and lag at r_{max} (**F:** lag%). Violin plots: each colored circle represents one participant; thick lines represent mean values; white circles indicate median values; dark areas indicate quartiles.*

An average of 5.9 ± 1.1 NoS was determined among participants. For tVAF1 a significant effect of TASK ($p < 0.001$) was observed. Post hoc comparisons revealed that tVAF1 was higher in BEAM compared to LINE ($p < 0.01$) and TIGHTROPE was higher than both LINE and BEAM ($p < 0.001$). There were no significant differences in tVAFNoS. Regarding the distinctness of activation coefficients, the ANOVA revealed a significant effect of TASK for r ($p < 0.05$), where activation coefficients were more correlated to each other ($p < 0.05$) in TIGHTROPE compared to LINE and BEAM. There was no significant difference for r_{max}, but a significant effect of TASK ($p < 0.001$) and TIME ($p < 0.05$) in lag%. The lag% was higher in LINE than BEAM ($p < 0.01$) and TIGHTROPE had the lowest %lag ($p < 0.001$) (Figure 2).

Trial-to-trial similarity measured by r and r_{max} was affected by TASK ($p < 0.001$) and TIME ($p < 0.01$). r and r_{max} was the highest in LINE, followed by BEAM (r_{max}: $p < 0.01$; $r < 0.001$) and lowest in TIGHTROPE (both: $p < 0.001$). Contrasts showed an increase in similarity from startBEAM to endBEAM (both: $p < 0.05$) and TRfail to TRsucc (r_{max}: $p < 0.05$; r: $p < 0.001$). There was no difference in lag% (Figure 3).

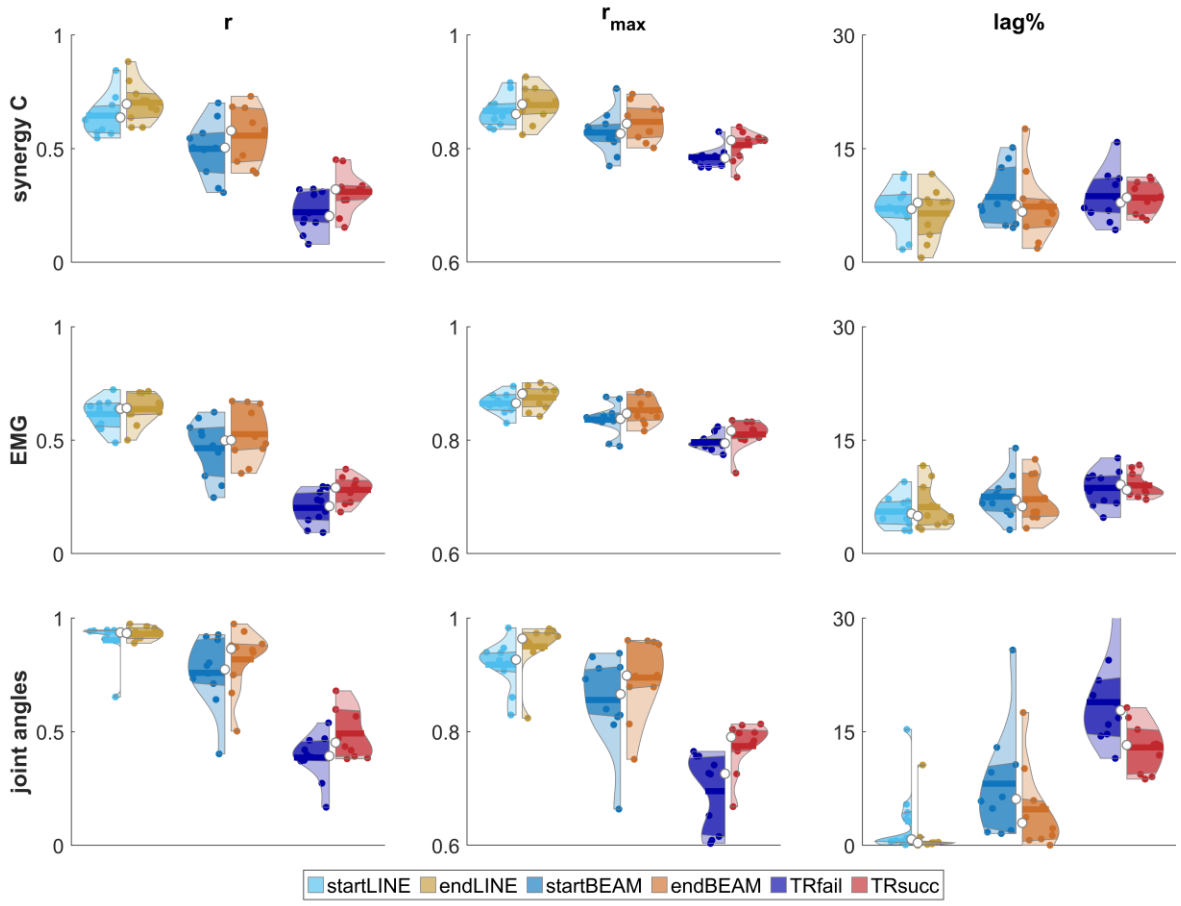

Figure 3: *Overall trial-to-trial similarity of synergy activation coefficients (C, top row), electromyography envelopes (EMG, middle row) and joint angles (bottom row), measured by Pearson correlation (r), maximum cross-correlation coefficient (r_{max}) and lag at r_{max} (lag%). Violin plots: each colored circle represents one participant; thick lines represent mean values; white circles indicate median values; dark areas indicate quartiles.*

Silhouette analyses yielded six clusters (Figure 4) which are indicated by # in the following paragraphs. Low tVAF values indicate low contribution of synergies to the condition. The tVAF of all clusters was significantly affected by TASK (#5: $p < 0.05$; #1, 3: $p < 0.01$; others: $p < 0.001$). In cluster 4, tVAF of BEAM was lower than LINE ($p < 0.05$) and the lowest in TIGHTROPE ($p < 0.001$). For the other clusters, tVAF of TIGHTROPE was higher than BEAM (#5, 6: $p < 0.05$; #2: $p < 0.001$) and LINE (#1, 3, 5: $p < 0.01$; #2, 6: $p < 0.001$). In BEAM it was higher than LINE (#2: $p < 0.01$). For cluster 2, ANOVA also revealed a

significant effect of TIME ($p < 0.05$), with lower tVAF in START compared to END, and the interaction TASK × TIME ($p < 0.01$). In cluster 6, contrasts showed a decrease of tVAF over time in BEAM ($p < 0.05$) (Figure 5).

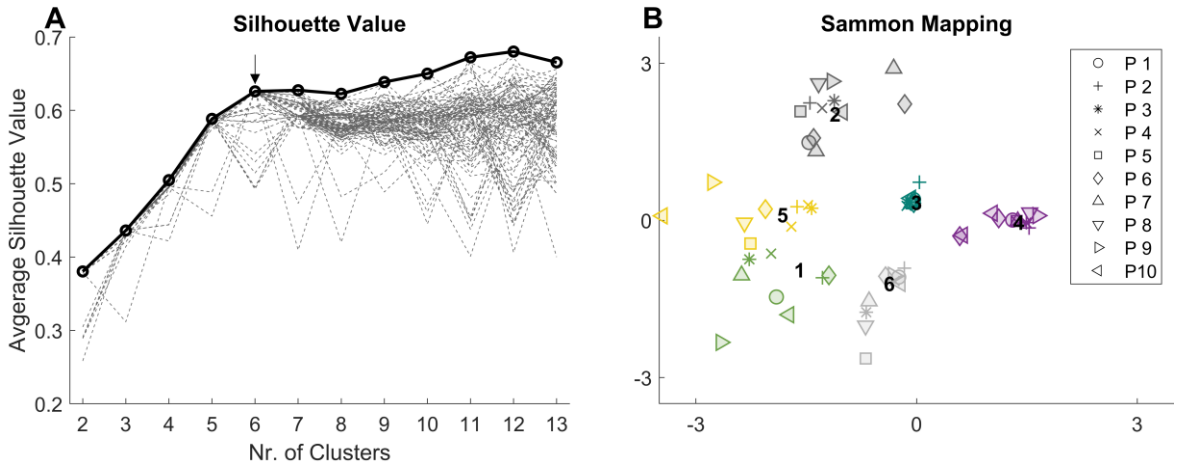

Figure 4: A: *dashed lines show the average silhouette value for each clustering repetition (1 to 100). The arrow indicates the number of clusters, at which the maximum of averaged silhouette values among repetitions (solid line/circles) plateaued.* ***B:*** *sammon mapping (Sammon, 1969) of the six clusters. Marker-styles indicate different participants (P1 – P10), and marker-colors indicate different clusters. Numbers (1 to 6) indicate the position of the clusters' centroids.*

Trial-to-trial similarity of cluster 1, 2, 4 and 5 was significantly affected by TASK in r and r_{max} (r_{max} #5: $p < 0.05$; r #5: $p < 0.01$ others: $p < 0.001$), with higher LINE than TIGHTROPE for r ($p < 0.001$) and r_{max} (#5: $p < 0.05$; others: $p < 0.001$) and higher BEAM than TIGHTROPE for r (#5 $p < 0.01$; others: $p < 0.001$). r_{max} was higher in BEAM than TIGHTROPE in cluster 1 ($p < 0.01$), 2 and 4 ($p < 0.001$). Correlation was higher in LINE than BEAM in cluster 1, 2 (r and r_{max}: $p < 0.05$) and 4 (r: $p < 0.01$; r_{max}: $p < 0.001$). The lag% revealed a significant effect of TASK for cluster 1, 3, 4 and 5(#3: $p < 0.05$; #5: $p < 0.05$; #1, 4: $p < 0.001$). LINE had lower lag% than BEAM (#1: $p < 0.05$) and TIGHTROPE (#5: $p < 0.01$; #1, 4: $p < 0.001$). BEAM had lower lag% compared to TIGHTROPE (#1, 5: $p < 0.01$). Contrary, #3 had the lowest lag% in TIGHTROPE compared to the other two conditions ($p < 0.05$) (Figure 5, Figure 6).

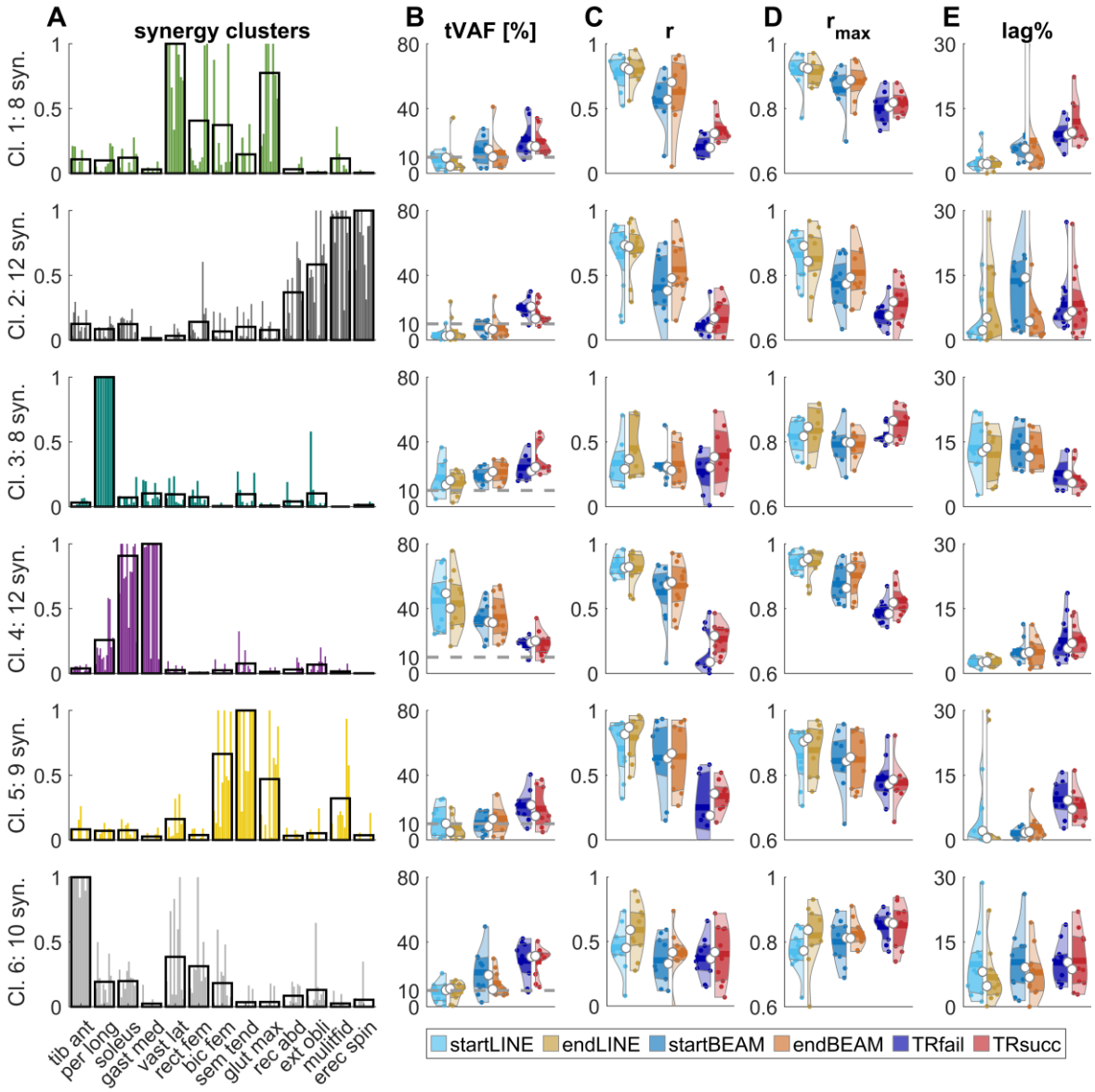

Figure 5: A: *muscle weightings of clustered synergies. Black borders are the cluster (Cl.) centroids, and colored bars (similar to Figure 4) represent the synergy vectors (syn.) that belong to this cluster.* ***B-E:*** *Violin plots represent the total variance accounted for (tVAF), pearson correlation coefficient (r), cross-correlation coefficient (r_{max}) and the lag-time (lag%) for each cluster. Violin plots: each colored circle represents one participant; thick lines represent mean values; white circles indicate median values; dark areas indicate quartiles.*

Significant effects of TIME were found for r in cluster 1 ($p < 0.05$), for r_{max} in cluster 4 and 6 ($p < 0.05$) and for lag% in cluster 4 ($p < 0.05$) with lower correlations and higher lag% in START compared to END. A significant effect of TASK × TIME was only found for r in cluster 4 ($p < 0.05$). Contrasts revealed a significant increase of r or r_{max} from startLINE to endLINE in cluster 6 (r_{max}: $p < 0.05$), from startBEAM to endBEAM in cluster 2 (r: $p < 0.01$) and from TRfail to TRsucc in cluster 1 (r: $p < 0.05$) (Figure 5, Figure 6).

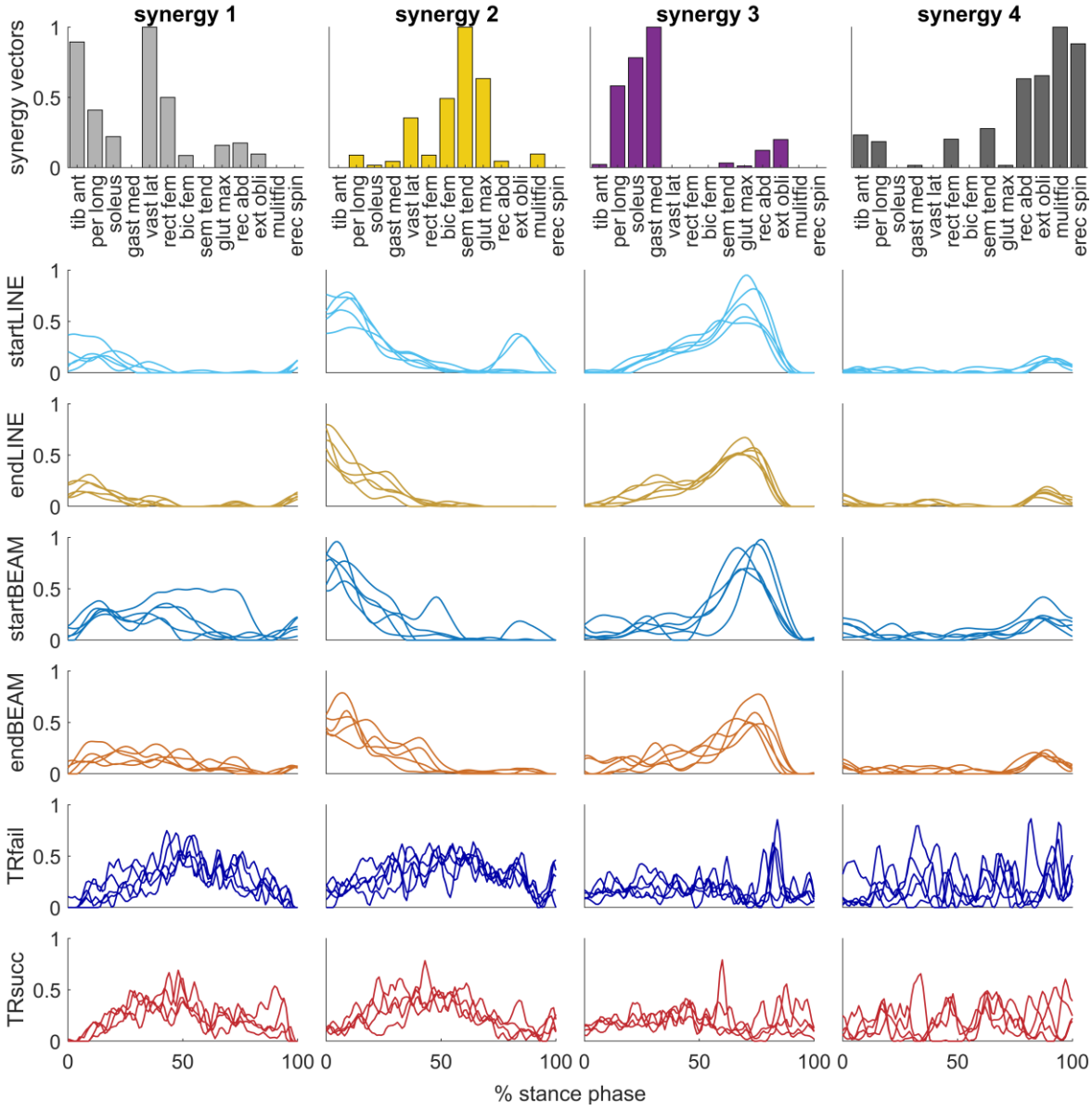

Figure 6: *All extracted synergy vectors (bar plots) and corresponding activation coefficients (waveform plots in the same column) for each condition of one participant (P8). Each waveform represents the activation coefficient of one trial. Bar colors indicate the cluster, which the motor module belongs to, and are the same as in Figure 4 and Figure 5.*

3.2 EMG analysis

Overall trial-to-trial similarity of EMG envelopes measured by r and r_{max} was significantly affected by TASK ($p < 0.001$), with LINE showing the highest correlation, followed by BEAM, and TIGHTROPE at last (r LINE vs BEAM: $p < 0.01$; others: $p < 0.001$). TIME influenced r ($p < 0.01$) and r_{max} ($p < 0.05$) and contrasts revealed lower r and r_{max} ($p < 0.05$) for startBEAM compared to endBEAM, and an increase in r ($p < 0.01$) between TRfail and TRsucc. The lag% was significantly affected by TASK ($p < 0.01$), with higher values in TIGHTROPE compared to LINE ($p < 0.01$). (Figure 3, Figure 7).

The amount of muscle activation measured by RMS revealed a significant effect of TASK, in all muscles, apart from soleus (glut_max: $p < 0.01$; others: $p < 0.001$). RMS of gast_med was lower in TIGHTROPE than BEAM ($p < 0.05$) and LINE ($p < 0.001$). For the other muscles, RMS was higher in TIGHTROPE than BEAM (glut_max: $p < 0.05$; tib_ant, bic_fem: $p < 0.01$; others: $p < 0.001$) and LINE ($p < 0.001$). In four muscles BEAM was also higher than LINE (rect_fem, multifid: $p < 0.05$; per_long, erec_spin: $p < 0.01$). There was a significant effect of TIME (rect_fem; bic_fem, glut_max: $p < 0.05$; tib_ant soleus, gast_med, sem_tend, erec_spin: $p < 0.01$; vast_lat, rec_abd, ext_obli: $p < 0.001$), and TASK × TIME (ext_obli: $p < 0.05$; tib_ant, vast_lat, sem_tend: $p < 0.01$; rec_abd, multifid, erec_spin: $p < 0.001$) on muscle activations. Contrasts revealed a higher muscle activation in startLINE than endLINE for two muscles (gast_med: $p < 0.05$, sem_tend: $p < 0.01$), startBEAM than endBEAM for four muscles (soleus, rect_fem, rec_abd: $p < 0.05$; tib_ant: $p < 0.01$), and TRfail than TRsucc for ten muscles (tib_ant, soleus, gast_med, erec_spin: $p < 0.01$; vast_lat, sem_tend, glut_max, rec_abd, ext_obli, multifid: $p < 0.001$) (Table 1).

Table 1: *Muscle activations (root-mean-square) for all conditions and muscles. M and SD represent the mean and standard deviation values across all participants. ANOVA revealed significant effects of TASK in all muscles apart from soleus. Significant differences observed by contrasts are indicated by *.*

	LINE				**BEAM**				**TIGHTROPE**			
	start		**end**		**start**		**end**		**fail**		**succ**	
	M	*SD*	*M*	*SD*	*M*	*SD*	*M*	*SD*	*M*	*SD*	*M*	*SD*
tib_ant	0.13	0.07	0.14	0.07	0.22*	0.09	0.16*	0.07	0.33*	0.07	0.27*	0.08
per_long	0.19	0.05	0.17	0.05	0.24	0.04	0.23	0.04	0.37	0.06	0.35	0.07
soleus	0.26	0.07	0.23	0.07	0.27*	0.06	0.24*	0.04	0.31*	0.10	0.25*	0.08
gast_med	0.32*	0.06	0.29*	0.06	0.29	0.05	0.27	0.05	0.24*	0.08	0.20*	0.06
vast_lat	0.14	0.09	0.12	0.07	0.17	0.10	0.15	0.08	0.32*	0.07	0.24*	0.08
rect_fem	0.05	0.03	0.04	0.02	0.07*	0.04	0.06*	0.02	0.21	0.09	0.17	0.08
bic_fem	0.09	0.05	0.08	0.07	0.11	0.07	0.11	0.08	0.25	0.08	0.20	0.09
sem_tend	0.17*	0.09	0.13*	0.08	0.17	0.08	0.16	0.09	0.29*	0.08	0.20*	0.08
glut_max	0.12	0.05	0.11	0.04	0.15	0.06	0.15	0.05	0.22*	0.09	0.18*	0.08
rec_abd	0.03	0.03	0.02	0.03	0.05*	0.05	0.04*	0.03	0.17*	0.08	0.10*	0.08
ext_obli	0.05	0.03	0.04	0.02	0.09	0.06	0.07	0.03	0.23*	0.07	0.17*	0.07
multifid	0.12	0.04	0.14	0.06	0.17	0.04	0.16	0.07	0.28*	0.04	0.21*	0.06
erec_spin	0.05	0.02	0.05	0.03	0.10	0.04	0.08	0.05	0.29*	0.03	0.20*	0.05

3.3 Kinematic analysis

Overall trial-to-trial similarity of joint angles, quantified by r, r_{max} and lag%, was significantly affected by TASK ($p < 0.001$). LINE exhibited the highest correlations and lowest lag%, followed by BEAM, and TIGHTROPE (r_{max} LINE vs BEAM: $p < 0.01$; lag% LINE vs BEAM: $p < 0.05$; others: $p < 0.001$). There was a significant effect of TIME on r ($p < 0.05$), with lower r in START compared to END, and a significant interaction effect of TASK × TIME ($p < 0.05$). For r_{max}, TIME had a significant effect ($p < 0.01$), with an increase observed between START and END. All contrasts were significant ($p < 0.05$). Likewise, lag% was significantly influenced by TIME ($p < 0.01$). Contrasts revealed higher lag% in startLINE and TRfail compared to endLINE and TRsucc, respectively ($p < 0.05$) (Figure 3, Figure 7).

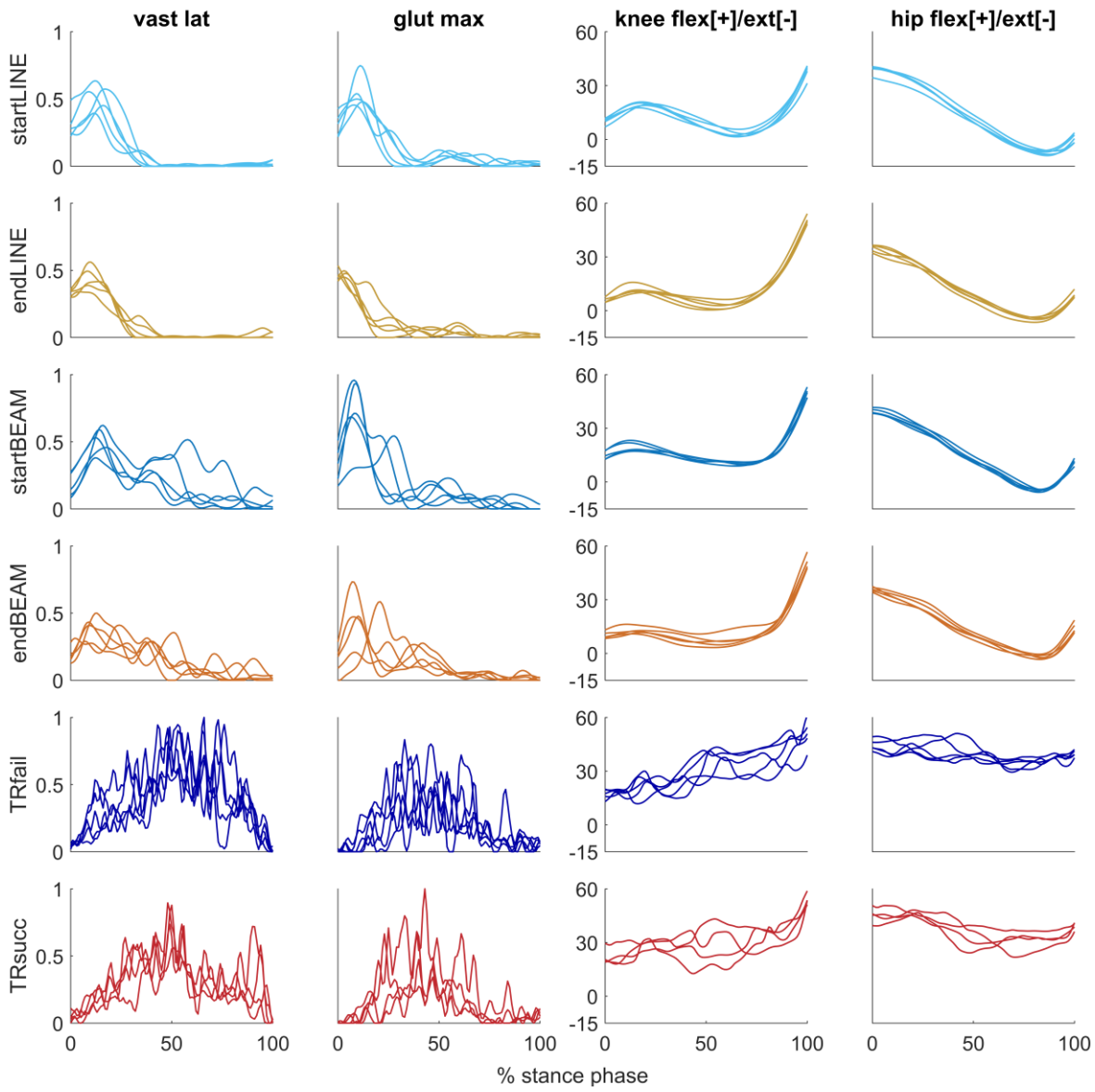

Figure 7: *Muscle activation (example of two muscles) and joint angle waveforms (example of two joint angles) from one participant (P8). Each waveform represents one trial per condition. vast lat = vastus lateralis; glut max = gluteus maximus; flex = flexion; ext = extension.*

4 Discussion

The aim of the study was to increase our insights in motor learning using synergy analysis by employing a within-participant, within-session study design. We observed higher distinctness and trial-to-trial similarity of activation coefficients with increasing movement proficiency. Furthermore, the analyses revealed that the contribution of specific synergies varies across tasks, and muscle activity decrease throughout the learning process.

Over half a century ago Bernstein (1967) proposed, that people restrict the number of degrees of freedom to simplify coordination in early learning stages. Steele et al. (2015) found higher overlapping of synergy activation coefficients with the occurrence of biomechanical and task constraints. The current study showed higher tVAF1 and overlapping of synergy recruitment – both indicating higher coactivation of synergy vectors – in movements with lower proficiency. Taken these findings together, we suggest that freezing the number of degrees of freedom in early learning is a result of coactivating synergy vectors. In consequence, high tVAF values might be caused by overlapping synergy activations and not necessarily mean a simpler motor control due to a decreased number of synergies. This theory is supported by previous studies on impaired and unimpaired populations. Clark et al. (2010) found similar synergy vectors in locomotion for stroke survivors and unimpaired individuals, if the same number of synergies were extracted, rather than the number determined by a tVAF threshold. The authors concluded that not the spatially synergy vectors differ, but they were computationally merged through the factorization algorithm due to their overlapping recruitment profiles. Similarly, merging of synergy vectors was found in locomotion of individuals post-stroke (Mizuta et al., 2022) and with Parkinson's disease (Ghislieri et al., 2023), and in reaching tasks after cortical lesions (Cheung et al., 2012). A higher amount of shared synergies between overground walking and balancing tasks was found in expert dancers compared to individuals with no dancing experience (Allen et al., 2020; Sawers et al., 2015), in post-stroke survivors compared to unimpaired individuals (Allen et al., 2019), and after a dance-based rehabilitation in individuals with Parkinson's disease (Allen et al., 2017). Two of these studies (Allen et al., 2017; Sawers et al., 2015) also found lower distinctness of synergy vectors in groups with fewer shared synergies. The lower distinctness of computed vectors may be a result of higher overlapping of activation coefficients, which can compromise the accuracy of extracted synergy vectors. This phenomenon has been observed in previous studies on real and simulated datasets (Soomro et al., 2018; Steele, Tresch, et al., 2015; Tresch et al., 2006), where increased temporal overlap of activation

coefficients led to merging of synergies due to the underlying assumptions of factorization algorithms. Consequently, these inaccurately extracted synergy vectors could explain the lower number of shared synergies. In the current study we also found a low number of shared synergies when computing them separately for each condition, but similar synergies when computing them over all conditions (see appendix). This suggests that with proficiency overlapping of activation coefficients reduced, rather than the number of shared synergies changed. This concept should be addressed in further studies.

An important feature of motor learning is motion fusion, also called coarticulation, which describes the combination of individual movement primitives into a smooth action. More precisely, the velocity peaks of two movements gradually disappear during learning. Typically, motion fusion is assessed by examining velocity peaks in hand trajectories during tasks that involve precise movements, such as following a specific curvature on a monitor. (Flash & Hochner, 2005; Friedman & Korman, 2019; Sosnik et al., 2004; Sporn et al., 2022). At first glance, our findings of higher activation distinctness with proficiency may seem to contradict the concept of motion fusion. However, further analysis (results not presented) revealed that the timing of velocity peaks in knee and ankle flexion/extension became more synchronized with higher proficiency. This suggests that improved coordination of synergy activation timing leads to motion fusion and ultimately results in smoother movements. Even thought we did not find significant changes in tVAF1 and distinctness between TRfail and TRsucc, these factors might change during learning and were potentially not significantly affected in the current study due to still quite low movement proficiency (4 out of 5 successful attempts) after learning.

Analysis on muscle activations revealed that all muscles apart of the gastrocnemius medialis were more activated in TIGHTROPE compared to LINE and BEAM. Moreover, the amount of activation was higher in TRfail than TRsucc for most muscles (Table 1). A decrease in muscle activity during learning has previously been observed (Donath et al., 2013; Donath et al., 2016). Keller et al. (2012) found reduced H-reflexes after a slackline training, which could explain less muscle activity with higher proficiency, due to less coactivation of agonist and antagonist muscles among a joint. In addition to this feedback-theory, we introduce a feedforward-approach. Our assumption is that synergies that are relevant for specific subtasks at a given time need to dominate over other synergies that may be activated at similar timings but are irrelevant to those subtasks. As proficiency increases and there is

higher distinctness among activation coefficients, synergies for the relevant subtasks can be less activated.

The current study revealed a decrease of trial-to-trial variability during learning, and with higher proficiency (Figure 3). These findings strengthen previous studies on trial-to-trial variability as outlined in the introduction (Cardis et al., 2018; Cheung, Zheng, et al., 2020; Dhawale et al., 2017; Levy-Tzedek, 2017; Sawers et al., 2015; Sylos-Labini et al., 2022; Wu et al., 2014). Regarding the overall trial-to-trial similarity of synergy vectors, we found a transfer effect of a balancing training on the TIGHTROPE to the BEAM. However, there were no differences between startLINE and endLINE suggesting that differences did not occur due to movement-artefacts or sensor-noise. Through cluster analysis we were able to detect whether changes in variability happen in all synergy vectors and interestingly, cluster 6 did not reveal any changes in variability due to proficiency or learning. Surprisingly, in cluster 3, lag% was lowest in TIGHTROPE. An explanation could be, that in order to perform a step, regardless of the task and proficiency, activation patterns of these synergy vectors have to be quite specific and do not allow much trial-to-trial variability. On basis of our analyses, we can only speculate about this feature. The other clusters showed that trial-to-trial similarity increases with movement proficiency. While we observed an increase of trial-to-trial similarity from startBEAM to endBEAM and from TRfail to TRsucc in certain clusters, other clusters showed no changes throughout the learning process. This suggests that early learning is driven by an increase in the consistency of certain synergies, while other synergies increase their consistency during a later learning stage, i.e.: with higher proficiency levels. A noteworthy finding from the cluster analysis was that high trial-to-trial variability did not necessarily correspond to the contributions of synergies to the task. While most synergies contributed more in TIGHTROPE, cluster 4 - primarily formed by shank muscles - actually contributed more in LINE. Interestingly, despite its higher contribution in LINE, cluster 4 also exhibited the highest trial-to-trial variability in TIGHTROPE (Figure 5).

For a more comprehensive understanding of changes in trial-to-trial variability, we also examined variability of EMG envelopes and joint angles (Figure 3). Overall EMG and joint angle variability were similar to overall synergy variability regarding task proficiency. Surprisingly, overall trial-to-trial similarity of kinematic data was not only higher with proficiency and after learning, but also in endLINE compared to startLINE. Therefore, we hypothesize that synergies reflect motor planning through the central nervous system, while

kinematics are more affected by peripherical noise in the movement execution (Dhawale et al., 2017; Faisal et al., 2008).

Stance phases duration differed between tasks and between TRsucc and TRfail. Namely, stance phases were shorter in TRsucc than TRfail (appendix). This explains the smoother synergy activation patterns in LINE and BEAM compared to TIGHTROPE (Hug, 2011) (Figure 6). One could assume higher trial-to-trail variability in TIGHTROPE as a result of less smoothed activation coefficients, but this would not explain variability differences between LINE and BEAM, as stance duration was not different between these two tasks. To further evaluate if our findings were affected by the different task durations, we modified the low-pass cutoff frequency for each trial, based on its duration and repeated our main analyses on synergies. Detailed information and results for the additional analyses are provided in the appendix. Briefly, these analyses showed similar results according to trial-to-trial similarity and distinctness between the tasks. However, when comparing TRfail to TRsucc, not only trial-to-trial similarity, but also distinctness of activation coefficients revealed an increase. In summary, we drew the same conclusions based on the additional and the main analyses. Namely, fine tuning of synergy recruitment, i.e. increasing trial-to-trial similarity and activation distinctness, is important for motor learning. We hypothesize that after a more completed learning process (i.e. all attempts of TIGHTROPE walking are successful) both will increase even more and precede similar levels like BEAM and LINE.

In the field of motor learning and development three theories are widely discussed (Sylos-Labini et al., 2022). The strict nativist view proposes that locomotor modules remain robustly conserved into adulthood, supported by the spatial synergy model (Ghislieri et al., 2023; Turpin et al., 2021) and studies observing basic stepping patterns in newborns (Ivanenko et al., 2013). The learning hypothesis suggests that unstructured movement patterns are transformed into structured solutions during development through the interaction between the body and the environment, evidenced by studies showing high trial-to-trial variability in early learning (Cardis et al., 2018; Cheung, Zheng, et al., 2020; Dhawale et al., 2017; Levy-Tzedek, 2017; Sawers et al., 2015; Sylos-Labini et al., 2022; Wu et al., 2014). A combined approach posits the existence of conserved movement patterns enriched with new patterns to represent a wider range of tasks. This concept has been recently supported by muscle synergy analysis in locomotion development (Sylos-Labini et al., 2022). In line with this, Cheung et al. (2020) observed both, consistent and variable synergies during running development. Here, we found similar synergy vectors across tasks. In a

subsequently analysis we confirmed this finding, by extracting synergy vectors separately for each condition. Briefly we found that similar motor control was utilized for all tasks. A more detailed discussion of this analysis is provided in the appendix. Beside similar synergy vectors, we observed higher variability in their activations in low proficiency levels. Furthermore, certain synergy vectors showed minimal contribution to LINE and BEAM tasks but were important for TIGHTROPE, indicating an enrichment of the motor control repertoire. These findings provide support for the combined nativist and learning theory.

Our study included two notable limitations. Firstly, due to the intra-session design, we captured a limited number of gait cycles per condition. Oliveira et al. (2014) suggested to extract muscle synergies over a minimum of 20 concatenated steps to account for trial-to-trial variability in movement execution. To address this, we performed our main analysis on concatenated data of all conditions, providing a larger sample size of 24 to 30 stance phases per participant. Secondly, we considered the learning process to be complete when participants successfully walked across the entire tightrope in four out of five consecutive attempts, which may not reflect a high level of proficiency. Nonetheless, despite this limitation, we observed significant changes from TRfail to TRsucc in most analyzed parameters.

In summary, our study aimed to investigate motor learning using synergy analysis through a within-session, within-participant study design. We found that increasing movement proficiency led to higher distinctness and trial-to-trial similarity of synergy activation coefficients. Our findings suggest that freezing the number of degrees of freedom in early learning is a result of higher temporal overlap of synergy recruitment. Furthermore, our results support the notion that variability during the learning process increases the likelihood of finding the optimal motor command. We conclude that finetuning of synergy recruitment is crucial for motor learning.

5 References

Allen, J. L., Carey, H. D., Ting, L. H., & Sawers, A. (2020). Generalization of motor module recruitment across standing reactive balance and walking is associated with beam walking performance in young adults. *Gait Posture*, *82*, 247. https://doi.org/10.1016/j.gaitpost.2020.09.016

Allen, J. L., Kesar, T. M., & Ting, L. H. (2019). Motor module generalization across balance and walking is impaired after stroke. *J Neurophysiol*, *122*, 289. https://doi.org/10.1152/jn.00561.2018

Allen, J. L., McKay, J. L., Sawers, A., Hackney, M. E., & Ting, L. H. (2017). Increased neuromuscular consistency in gait and balance after partnered, dance-based rehabilitation in parkinson's disease. *J Neurophysiol*, *118*, 373. https://doi.org/10.1152/jn.00813.2016

Atif, S. M., Qazi, S., & Gillis, N. (2019). Improved SVD-based initialization for nonnegative matrix factorization using low-rank correction. *Pattern recognition letters*, *122*, 59. https://doi.org/10.1016/j.patrec.2019.02.018

Ballarini, R., Ghislieri, M., Knaflitz, M., & Agostini, V. (2021). An algorithm for choosing the optimal number of muscle synergies during walking. *Sensors (Basel, Switzerland)*, *21*. https://doi.org/10.3390/s21103311

Banks, C. L., Pai, M. M., McGuirk, T. E., Fregly, B. J., & Patten, C. (2017). Methodological choices in muscle synergy analysis impact differentiation of physiological characteristics following stroke. *Front Comput Neurosci*, *11*, 78. https://doi.org/10.3389/fncom.2017.00078

Barroso, F. O., Torricelli, D., Moreno, J. C., Taylor, J., Gomez-Soriano, J., Bravo-Esteban, E., . . . Pons, J. L. (2014). Shared muscle synergies in human walking and cycling. *J Neurophysiol*, *112*, 1998. https://doi.org/10.1152/jn.00220.2014

Bernstein, N. (1967). The Coordination and Regulation of Movements. In. New York: Perganmon Press.

Bianco, N. A., Patten, C., & Fregly, B. J. (2018). Can Measured Synergy Excitations Accurately Construct Unmeasured Muscle Excitations? *J Biomech Eng*, *140*(1). https://doi.org/10.1115/1.4038199

Bizzi, E., & Cheung, V. C. K. (2013). The neural origin of muscle synergies. *Front Comput Neurosci*, *7*, 6. https://doi.org/10.3389/fncom.2013.00051

Bizzi, E., Tresch, M. C., & Saltiel, P. (1999). The construction of movement by the spinal cord. *Nat Neurosci*, *2*, 167. https://doi.org/10.1038/5721

Boccia, G., Zoppirolli, C., Bortolan, L., Schena, F., & Pellegrini, B. (2018). Shared and task-specific muscle synergies of Nordic walking and conventional walking. *Scand J Med Sci Sports*, *28*, 918. https://doi.org/10.1111/sms.12992

Boutsidis, C., & Gallopoulos, E. (2008). SVD based initialization: A head start for nonnegative matrix factorization. *Pattern recognition*, *41*, 1362. https://doi.org/10.1016/j.patcog.2007.09.010

Cardis, M., Casadio, M., & Ranganathan, R. (2018). High variability impairs motor learning regardless of whether it affects task performance. *J Neurophysiol*, *119*, 48. https://doi.org/10.1152/jn.00158.2017

Cheung, V. C. K., Cheung, B. M. F., Zhang, J. H., Chan, Z. Y. S., Ha, S. C. W., Chen, C.-Y., & Cheung, R. T. H. (2020). Plasticity of muscle synergies through fractionation and merging during development and training of human runners. *Nature Communications*, *11*(1), 4356. https://doi.org/10.1038/s41467-020-18210-4

Cheung, V. C. K., Turolla, A., Agostini, M., Silvoni, S., Bennis, C., Kasi, P., . . . Bizzi, E. (2012). Muscle synergy patterns as physiological markers of motor cortical damage. *Proc Natl Acad Sci U S A*, *109*, 14656. https://doi.org/10.1073/pnas.1212056109

Cheung, V. C. K., Zheng, X.-C., Cheung, R. T. H., & Chan, R. H. M. (2020). Modulating the Structure of Motor Variability for Skill Learning Through Specific Muscle Synergies in Elderlies and Young Adults. *IEEE Open J Eng Med Biol*, *1*, 40. https://doi.org/10.1109/OJEMB.2019.2963666

Chvatal, S. A., & Ting, L. H. (2013). Common muscle synergies for balance and walking. *Front Comput Neurosci*, *7*, 48. https://doi.org/10.3389/fncom.2013.00048

Chvatal, S. A., Torres-Oviedo, G., Safavynia, S. A., & Ting, L. H. (2011). Common muscle synergies for control of center of mass and force in nonstepping and stepping postural behaviors. *J Neurophysiol*, *106*, 1015. https://doi.org/10.1152/jn.00549.2010

Clark, D. J., Ting, L. H., Zajac, F. E., Neptune, R. R., & Kautz, S. A. (2010). A. Merging of healthy motor modules predicts reduced locomotor performance and muscle coordination complexity post-stroke. *J Neurophysiol*, *103*, 857. https://doi.org/10.1152/jn.00825.2009

d'Avella, A., & Bizzi, E. (2005). Shared and Specific Muscle Synergies in Natural Motor Behaviors. *Proc Natl Acad Sci U S A*, *102*, 3081. https://doi.org/10.1073/pnas.0500199102

da Silva Costa, A. A., Moraes, R., Hortobágyi, T., & Sawers, A. (2020). Older adults reduce the complexity and efficiency of neuromuscular control to preserve walking balance. *Exp Gerontol*, *140*, 111050. https://doi.org/10.1016/j.exger.2020.111050

Delp, S. L., Anderson, F. C., Arnold, A. S., Loan, P., Habib, A., John, C. T., . . . Thelen, D. G. (2007). OpenSim: open-source software to create and analyze dynamic simulations of movement. *IEEE Trans Biomed Eng*, *54*(11), 1940-1950. https://doi.org/10.1109/tbme.2007.901024

Dhawale, A. K., Smith, M. A., & Ölveczky, B. P. (2017). The Role of Variability in Motor Learning. *Annu Rev Neurosci*, *40*, 498. https://doi.org/10.1146/annurev-neuro-072116-031548

Dominici, N., Ivanenko, Y. P., Cappellini, G., d'Avella, A., Mondì, V., Cicchese, M., . . . Lacquaniti, F. (2011). Locomotor primitives in newborn babies and their development. *Science*, *334*(6058), 997-999. https://doi.org/10.1126/science.1210617

Donath, L., Roth, R., Rueegge, A., Groppa, M., Zahner, L., & Faude, O. (2013). Effects of slackline training on balance, jump performance & muscle activity in young children. *Int J Sports Med*, *34*, 1098. https://doi.org/10.1055/s-0033-1337949

Donath, L., Roth, R., Zahner, L., & Faude, O. (2016). Slackline training and neuromuscular performance in seniors: A randomized controlled trial. *Scand J Med Sci Sports*, *26*, 283. https://doi.org/10.1111/sms.12423

Eaton, J. W., Bateman, D., Hauberg, S., & Wehbring, R. (2021). *GNU Octave version 6.2.0 manual: a high-level interactive language for numerical computations*. URL https://www.gnu.org/software/octave/doc/v6.2.0/

Elkin, L. A., Kay, M., Higgins, J. J., & Wobbrock, J. O. (2021). An Aligned Rank Transform Procedure for Multifactor Contrast Tests. 768. https://doi.org/10.1145/3472749.3474784

Faisal, A. A., Selen, L. P. J., & Wolpert, D. M. (2008). Noise in the nervous system. *Nat Rev Neurosci*, *9*, 303. https://doi.org/10.1038/nrn2258

Flash, T., & Hochner, B. (2005). Motor primitives in vertebrates and invertebrates. *Curr Opin Neurobiol*, *15*, 666. https://doi.org/10.1016/j.conb.2005.10.011

Frey Law, L., Krishnan, C., & Avin, K. (2010). Modeling nonlinear errors in surface electromyography due to baseline noise: A new methodology. *J Biomech*, *44*, 205. https://doi.org/10.1016/j.jbiomech.2010.09.008

Friedman, J., & Korman, M. (2019). Observation of an expert model induces a skilled movement coordination pattern in a single session of intermittent practice. *Sci Rep*, *9*, 4609. https://doi.org/10.1038/s41598-019-40924-9

Frère, J., & Hug, F. (2012). Between-subject variability of muscle synergies during a complex motor skill [Original Research]. *Frontiers in Computational Neuroscience*, *6*(99). https://doi.org/10.3389/fncom.2012.00099

Ghislieri, M., Lanotte, M., Knaflitz, M., Rizzi, L., & Agostini, V. (2023). Muscle synergies in Parkinson's disease before and after the deep brain stimulation of the bilateral subthalamic nucleus. *Sci Rep*, *13*, 6997. https://doi.org/10.1038/s41598-023-34151-6

Gizzi, L., Nielsen, J. F., Felici, F., Ivanenko, Y. P., & Farina, D. (2011). Impulses of activation but not motor modules are preserved in the locomotion of subacute stroke patients. *J Neurophysiol*, *106*, 210. https://doi.org/10.1152/jn.00727.2010

Hagio, S., Fukuda, M., & Kouzaki, M. (2015). Identification of muscle synergies associated with gait transition in humans. *Front Hum Neurosci*, *9*, 48. https://doi.org/10.3389/fnhum.2015.00048

Heales, L. J., Hug, F., MacDonald, D. A., Vicenzino, B., & Hodges, P. W. (2016). Is synergistic organisation of muscle coordination altered in people with lateral epicondylalgia? A case–control study. *Clin Biomech (Bristol, Avon)*, *35*, 131. https://doi.org/10.1016/j.clinbiomech.2016.04.017

Hiep Vu Nguyen, S., Nambu, I., & Wada, Y. (2016, 9-12 Oct. 2016). The adjustment of muscle synergy recruitment by controlling muscle contraction during the reaching movement. 2016 IEEE International Conference on Systems, Man, and Cybernetics (SMC),

Higgins, J., Blair, R., & Tashtoush, S. (1990). THE ALIGNED RANK TRANSFORM PROCEDURE. *Conference on Applied Statistics in Agriculture*. https://doi.org/10.4148/2475-7772.1443

Huebner, A., Faenger, B., Scholle, H.-C., & Anders, C. (2015). Re-evaluation of the amplitude–force relationship of trunk muscles. *J Biomech*, *48*, 1205. https://doi.org/10.1016/j.jbiomech.2015.02.016

Hug, F. (2011). Can muscle coordination be precisely studied by surface electromyography? *J Electromyogr Kinesiol*, *21*, 12. https://doi.org/10.1016/j.jelekin.2010.08.009

Hug, F., Turpin, N. A., Couturier, A., & Dorel, S. (2011). Consistency of muscle synergies during pedaling across different mechanical constraints. *J Neurophysiol*, *106*(1), 91-103. https://doi.org/10.1152/jn.01096.2010

Hug, F., Turpin, N. A., Dorel, S., & Guével, A. (2012). Smoothing of electromyographic signals can influence the number of extracted muscle synergie. *Clin Neurophysiol*, *123*, 1896. https://doi.org/10.1016/j.clinph.2012.01.015

Hug, F., Vogel, C., Tucker, K., Dorel, S., Deschamps, T., Le Carpentier, É., & Lacourpaille, L. (2019). Individuals have unique muscle activation signatures as revealed during gait and pedaling. *J Appl Physiol (1985)*, *127*, 1174. https://doi.org/10.1152/japplphysiol.01101.2018

Ivanenko, Y. P., Dominici, N., Cappellini, G., Di Paolo, A., Giannini, C., Poppele, R. E., & Lacquaniti, F. (2013). Changes in the spinal segmental motor output for stepping during development from infant to adult. *J Neurosci*, *33*, 36a. https://doi.org/10.1523/JNEUROSCI.2722-12.2013

Ivanenko, Y. P., Poppele, R. E., & Lacquaniti, F. (2004). Five basic muscle activation patterns account for muscle activity during human locomotion. *J Physiol*, *556*, 282. https://doi.org/10.1113/jphysiol.2003.057174

Kadaba, M. P., Ramakrishnan, H. K., & Wootten, M. E. (1990). Measurement of lower extremity kinematics during level walking. *J Orthop Res*, *8*(3), 383-392. https://doi.org/10.1002/jor.1100080310

Kaelbling, L. P., Littman, M. L., & Moore, A. W. (1996). Reinforcement learning: a survey. *arXiv.org*.

Keenon, W., Michael, R., Jon, S., Jennifer, L. H., Steve, C., Scott, L. D., & Liu, C. K. (2022). Rapid bilevel optimization to concurrently solve musculoskeletal scaling, marker registration, and inverse kinematic problems for human motion reconstruction. *bioRxiv*, 2022.2008.2022.504896. https://doi.org/10.1101/2022.08.22.504896

Keller, M., Pfusterschmied, J., Buchecker, M., Müller, E., & Taube, W. (2012). Improved postural control after slackline training is accompanied by reduced H-reflexes. *Scand J Med Sci Sports*, *22*, 477. https://doi.org/10.1111/j.1600-0838.2010.01268.x

Kieliba, P., Tropea, P., Pirondini, E., Coscia, M., Micera, S., & Artoni, F. (2018). How Are Muscle Synergies Affected by Electromyography Pre-Processing? *IEEE Trans Neural Syst Rehabil Eng*, *26*, 893. https://doi.org/10.1109/TNSRE.2018.2810859

Kim, J., & Park, H. (2008). *Toward Faster Nonnegative Matrix Factorization: A New Algorithm and Comparisons* Proceedings of the 2008 Eighth IEEE International Conference on Data Mining, https://doi.org/10.1109/ICDM.2008.149

Kim, Y., Bulea, T. C., & Damiano, D. L. (2016). Novel Methods to Enhance Precision and Reliability in Muscle Synergy Identification during Walking. *Front Hum Neurosci*, *10*, 455. https://doi.org/10.3389/fnhum.2016.00455

Kim, Y., Bulea, T. C., & Damiano, D. L. (2018). Children With Cerebral Palsy Have Greater Stride-to-Stride Variability of Muscle Synergies During Gait Than Typically Developing Children: Implications for Motor Control Complexity. *Neurorehabil Neural Repair*, *32*, 844. https://doi.org/10.1177/1545968318796333

Kristiansen, M., Samani, A., Madeleine, P., & Hansen, E. A. (2016). Muscle synergies during bench press are reliable across days. *J Electromyogr Kinesiol*, *30*, 88. https://doi.org/10.1016/j.jelekin.2016.06.004

Lee, D., & Seung, H. (2001). Algorithms for Non-negative Matrix Factorization. *Adv. Neural Inform. Process. Syst.*, *13*.

Levy-Tzedek, S. (2017). Motor errors lead to enhanced performance in older adults. *Sci Rep*, *7*, 8. https://doi.org/10.1038/s41598-017-03430-4

Meyer, A. J., Eskinazi, I., Jackson, J. N., Rao, A. V., Patten, C., & Fregly, B. J. (2016). Muscle Synergies Facilitate Computational Prediction of Subject-Specific Walking Motions. *Front Bioeng Biotechnol*, *4*, 77. https://doi.org/10.3389/fbioe.2016.00077

Mizuta, N., Hasui, N., Nishi, Y., Higa, Y., Matsunaga, A., Deguchi, J., . . . Morioka, S. (2022). Merged swing-muscle synergies and their relation to walking characteristics in subacute post-stroke patients: An observational study. *PLoS One*, *17*, e0263613. https://doi.org/10.1371/journal.pone.0263613

Muceli, S., Boye, A. T., D'Avella, A., & Farina, D. (2010). Identifying representative synergy matrices for describing muscular activation patterns during multidirectional reaching in the horizontal plane. *J Neurophysiol*, *103*, 1542. https://doi.org/10.1152/jn.00559.2009

Nazifi, M. M., Yoon, H. U., Beschorner, K., & Hur, P. (2017). Shared and task-specific muscle synergies during normal walking and slipping. *Front Hum Neurosci*, *11*, 40. https://doi.org/10.3389/fnhum.2017.00040

Ogihara, H., Tsushima, E., Kamo, T., Sato, T., Matsushima, A., Niioka, Y., . . . Azami, M. (2020). Kinematic gait asymmetry assessment using joint angle data in patients with chronic stroke—A normalized cross-correlation approach. *Gait Posture*, *80*, 173. https://doi.org/10.1016/j.gaitpost.2020.05.042

Oliveira, A. S., Gizzi, L., Farina, D., & Kersting, U. G. (2014). Motor modules of human locomotion: influence of EMG averaging, concatenation, and number of step cycles [Original Research]. *Frontiers in Human Neuroscience*, *8*. https://doi.org/10.3389/fnhum.2014.00335

Oliveira, A. S., Gizzi, L., Ketabi, S., Farina, D., & Kersting, U. G. (2016). Modular Control of Treadmill vs Overground Running. *PLoS One*, *11*, e0153307. https://doi.org/10.1371/journal.pone.0153307

Oshikawa, T., Adachi, G., Akuzawa, H., Okubo, Y., & Kaneoka, K. (2020). Electromyographic analysis of abdominal muscles during abdominal bracing and hollowing among six different positions. *JPFSM*, *9*, 163. https://doi.org/10.7600/jpfsm.9.157

Paatero, P., & Tapper, U. (1994). Positive matrix factorization: A non-negative factor model with optimal utilization of error estimates of data value“ . *Environmetrics*, *5*, 111-126.

Pale, U., Atzori, M., Müller, H., & Scano, A. (2020). Variability of muscle synergies in hand grasps: Analysis of intra-and inter-session data. *Sensors (Basel)*, *20*, 27. https://doi.org/10.3390/s20154297

Paterson, K. L., Hinman, R. S., Metcalf, B. R., Bennell, K. L., & Wrigley, T. V. (2017). Plug-in-Gait calculation of the knee adduction moment in people with knee osteoarthritis during shod walking: comparison of two different foot marker models. *J Foot Ankle Res*, *10*, 8. https://doi.org/10.1186/s13047-017-0187-4

Potvin, J. R., & Brown, S. H. M. (2004). Less is more: high pass filtering, to remove up to 99% of the surface EMG signal power, improves EMG-based biceps brachii muscle force estimates. *J Electromyogr Kinesiol*, *14*, 399. https://doi.org/10.1016/j.jelekin.2003.10.005

Profeta, V. L. S., & Turvey, M. T. (2018). Bernstein’s levels of movement construction: A contemporary perspective. *Hum Mov Sci*, *57*, 133. https://doi.org/10.1016/j.humov.2017.11.013

Rabbi, M. F., Pizzolato, C., Lloyd, D. G., Carty, C. P., Devaprakash, D., & Diamond, L. E. (2020). Non-negative matrix factorisation is the most appropriate method for extraction of muscle synergies in walking and running. *Sci Rep*, *10*, 8266. https://doi.org/10.1038/s41598-020-65257-w

Rajagopal, A., Dembia, C. L., DeMers, M. S., Delp, D. D., Hicks, J. L., & Delp, S. L. (2016). *Full-Body Musculoskeletal Model for Muscle-Driven Simulation of Human Gait*. *IEEE Trans Biomed Eng*, *63*, 2079. https://doi.org/10.1109/TBME.2016.2586891

Ranganathan, R., & Krishnan, C. (2012). Extracting synergies in gait: using EMG variability to evaluate control strategies. *J Neurophysiol*, *108*, 1544. https://doi.org/10.1152/jn.01112.2011

Rodriguez, K. L., Roemmich, R. T., Cam, B., Fregly, B. J., & Hass, C. J. (2013). Persons with Parkinson’s disease exhibit decreased neuromuscular complexity during gait. *Clin Neurophysiol*, *124*, 1397. https://doi.org/10.1016/j.clinph.2013.02.006

Roh, J., Rymer, W. Z., & Beer, R. F. (2012). Robustness of muscle synergies underlying three-dimensional force generation at the hand in healthy humans. *J Neurophysiol*, *107*, 2142. https://doi.org/10.1152/jn.00173.2011

Roh, J., Rymer, W. Z., Perreault, E. J., Yoo, S. B., & Beer, R. F. (2013). Alterations in upper limb muscle synergy structure in chronic stroke survivors. *J Neurophysiol*, *109*, 781. https://doi.org/10.1152/jn.00670.2012

Rousseeuw, P. J. (1987). Silhouettes: A graphical aid to the interpretation and validation of cluster analysis. *Journal of Computational and Applied Mathematics*, *20*, 53-65. https://doi.org/https://doi.org/10.1016/0377-0427(87)90125-7

Safavynia, S. A., & Ting, L. H. (2012). Task-level feedback can explain temporal recruitment of spatially fixed muscle synergies throughout postural perturbations. *J Neurophysiol*, *107*, 177. https://doi.org/10.1152/jn.00653.2011

Sammon, J. W. (1969). A Nonlinear Mapping for Data Structure Analysis. *IEEE transactions on computers*, *C-18*, 409. https://doi.org/10.1109/T-C.1969.222678

Sawers, A., Allen, J. L., & Ting, L. H. (2015). Long-term training modifies the modular structure and organization of walking balance control. *J Neurophysiol*, *114*, 3373. https://doi.org/10.1152/jn.00758.2015

Scano, A., Dardari, L., Molteni, F., Giberti, H., Tosatti, L. M., & d'Avella, A. (2019). A Comprehensive Spatial Mapping of Muscle Synergies in Highly Variable Upper-Limb Movements of Healthy Subjects [Original Research]. *Frontiers in Physiology*, *10*. https://doi.org/10.3389/fphys.2019.01231

Seung, H. S., & Lee, D. D. (1999). Learning the parts of objects by non-negative matrix factorization. *Nature*, *401*, 791. https://doi.org/10.1038/44565

Shuman, B. R., Schwartz, M. H., & Steele, K. M. (2017). Electromyography Data Processing Impacts Muscle Synergies during Gait for Unimpaired Children and Children with Cerebral Palsy [Original Research]. *Frontiers in Computational Neuroscience*, *11*(50). https://doi.org/10.3389/fncom.2017.00050

Soomro, M. H., Conforto, S., Giunta, G., Ranaldi, S., & De Marchis, C. (2018). Comparison of Initialization Techniques for the Accurate Extraction of Muscle Synergies from Myoelectric Signals via Nonnegative Matrix Factorization. *Appl Bionics Biomech*, *2018*, 10. https://doi.org/10.1155/2018/3629347

Sosnik, R., Hauptmann, B., Karni, A., & Flash, T. (2004). When practice leads to co-articulation: the evolution of geometrically defined movement primitives. *Exp Brain Res*, *156*, 438. https://doi.org/10.1007/s00221-003-1799-4

Sporn, S., Chen, X., & Galea, J. M. (2022). The dissociable effects of reward on sequential motor behavior. *J Neurophysiol*, *128*, 104. https://doi.org/10.1152/jn.00467.2021

Steele, K. M., Rozumalski, A., & Schwartz, M. H. (2015). Muscle synergies and complexity of neuromuscular control during gait in cerebral palsy. *Dev Med Child Neurol*, *57*, 1182. https://doi.org/10.1111/dmcn.12826

Steele, K. M., Tresch, M. C., & Perreault, E. J. (2015). Consequences of biomechanically constrained tasks in the design and interpretation of synergy analyses. *J Neurophysiol*, *113*, 2113. https://doi.org/10.1152/jn.00769.2013

Sylos-Labini, F., La Scaleia, V., Cappellini, G., Dewolf, A., Fabiano, A., Solopova, I. A., . . . Lacquaniti, F. (2022). Complexity of modular neuromuscular control increases and variability decreases during human locomotor development. *Communications Biology*, *5*(1), 1256. https://doi.org/10.1038/s42003-022-04225-8

Ting, L., & Chvatal, S. (2010). Decomposing Muscle Activity in Motor TasksMethods and Interpretation. In (pp. 102-138). https://doi.org/10.1093/acprof:oso/9780195395273.003.0005

Tresch, M. C., Cheung, V. C. K., & d'Avella, A. (2006). Matrix Factorization Algorithms for the Identification of Muscle Synergies: Evaluation on Simulated and Experimental Data Sets. *J Neurophysiol*, *95*, 2212. https://doi.org/10.1152/jn.00222.2005

Turpin, N. A., Costes, A., Moretto, P., & Watier, B. (2017). Can muscle coordination explain the advantage of using the standing position during intense cycling? *J Sci Med Sport*, *20*, 616. https://doi.org/10.1016/j.jsams.2016.10.019

Turpin, N. A., Uriac, S., & Dalleau, G. (2021). How to improve the muscle synergy analysis methodology? *Eur J Appl Physiol*, *121*, 1025. https://doi.org/10.1007/s00421-021-04604-9

Van Criekinge, T., Vermeulen, J., Wagemans, K., Schröder, J., Embrechts, E., Truijen, S., . . . Saeys, W. (2020). Lower limb muscle synergies during walking after stroke: a systematic review. *Disability and Rehabilitation*, *42*(20), 2836-2845. https://doi.org/10.1080/09638288.2019.1578421

van den Hoorn, W., van Dieen, J. H., Hodges, P. W., & Hug, F. (2015). Effect of acute noxious stimulation to the leg or back on muscle synergies during walking. *J Neurophysiol*, *113*, 54. https://doi.org/10.1152/jn.00557.2014

van der Krogt, M., Oudenhoven, L., Buizer, A., Dallmeijer, A., Dominici, N., & Harlaar, J. (2016). The effect of EMG processing choices on muscle synergies before and after BoNT-A treatment in cerebral palsy. *Gait & posture*, *49*, 31. https://doi.org/10.1016/j.gaitpost.2016.07.095

Vera-Garcia, F. J., Moreside, J. M., & McGill, S. M. (2009). MVC techniques to normalize trunk muscle EMG in healthy women. *J Electromyogr Kinesiol*, *20*, 16. https://doi.org/10.1016/j.jelekin.2009.03.010

Wobbrock, J., Findlater, L., Gergle, D., & Higgins, J. (2011). The Aligned Rank Transform for Nonparametric Factorial Analyses Using Only ANOVA Procedures. *Conference on Human Factors in Computing Systems*, 146. https://doi.org/10.1145/1978942.1978963

Wu, H. G., Miyamoto, Y. R., Castro, L. N. G., Ölveczky, B. P., & Smith, M. A. (2014). Temporal structure of motor variability is dynamically regulated and predicts motor learning ability. *Nat Neurosci*, *17*, 321. https://doi.org/10.1038/nn.3616

Yang, J. F., & Gorassini, M. (2006). Spinal and brain control of human walking: implications for retraining of walking. *Neuroscientist*, *12*, 389. https://doi.org/10.1177/1073858406292151

Zhao, K., Zhang, Z., Wen, H., & Scano, A. (2021). Intra-Subject and Inter-Subject Movement Variability Quantified with Muscle Synergies in Upper-Limb Reaching Movements. *Biomimetics (Basel, Switzerland)*, *6*. https://doi.org/10.3390/biomimetics6040063

Zheng, Z., Yang, J., & Zhu, Y. (2007). Initialization enhancer for non-negative matrix factorization. *Engineering applications of artificial intelligence*, *20*, 110. https://doi.org/10.1016/j.engappai.2006.03.001

6 List of Figures

7 List of Tables

Appendix

Synergy extraction – spatial synergy model

As mentioned in the main section, the spatial synergy model describes EMG signals as a linear combination of fixed synergy vectors and time dependent activation coefficients (Ghislieri et al., 2023; Profeta & Turvey, 2018; Turpin et al., 2021). The mathematical concept behind this, is presented in equation (1), where E is the EMG matrix, C the activation coefficient, W the synergy vector and e the residual error. Subscript *mus* indicates the number of muscles (here 13) and *tps* the number of timepoints (here the number of all trials per participant multiplied with 101). Note that k represents the number of extracted synergies and ranges from 1 to 12 (mus -1) in the current study, while g represents the synergy number (1 to k). The NNMF algorithm (Lee & Seung, 2001; Paatero & Tapper, 1994; Seung & Lee, 1999) aims to obtain the smallest possible residual error in this equation by updating C and W over numerous iterations.

$$(1) \quad E_{mus\times tps} = \sum_{g=1}^{k} C(g)_{k\times tps}\, W(g)_{mus\times k} + e$$

We used an advanced non-negative-matrix-factorization (NNMF) algorithm introduced by Kim & Park (Kim et al., 2016) based on the block principal pivoting method for the non-negativity constrained least squares problem. In this method, convergence is reached as a stop criterium, in contrast to the classic NNMF method which could get stuck in local minima. Hence, we used the "nmf_bpas" octave function where 50 to 5000 iterations were allowed, to reach a convergence criterium of 10^{-5} for f in equation (2). Both, α and β are the mean of E (but one could give each an individual initial guess instead), and the subscript F indicates the Frobenius norm.

$$(2) \quad f(W,C) = \frac{1}{2}(\|E - WC\|_F^2 + \alpha\, \|W\|_F^2 + \beta\|C\|_F^2$$

It has been shown, that the number of needed iterations at which a NNMF algorithm converges and its final solution is strongly affected by the initialization (= first guess) of W and C, that are - if not specified - random inputs (Atif et al., 2019; Boutsidis & Gallopoulos, 2008; Zheng et al., 2007). Recently, initialization methods like single-value-decompensation (SVD), principal-component-analysis, or spatial distributions gained some attention in muscle synergy analyzes due to their positive effects of hastening the NNMF algorithm and

performing better when activation coefficients of the different synergies are more correlated (Soomro et al., 2018; Turpin et al., 2021). Therefore, we here used the NNSVDLRC (nonnegative single-value-decompensation with low-rank correction) function introduced by Atif et al. (2019) with default inputs (stop criterion: 0.05; maximum number of iterations: 20) to obtain better initial guesses for W and C. This algorithm was designed for an improved performance on low ranks (k) which are important in muscle synergy analysis.

k-means clustering

As mentioned in the main section, we used octave's in-built "kmeans" function to cluster similar synergies among participants. The following properties were applied: squared Euclidean distance; k-means++ initialization algorithm; maximum iteration number of 10^{100} to reach a change of any centroid less than 0.0001; 5000 replicates.

Task duration

Methods

Previous studies found shorter gait-cycle durations after locomotor development (Ivanenko et al., 2013; Sylos-Labini et al., 2022; Yang & Gorassini, 2006). To evaluate if stance-phase durations were shorter with higher proficiency and after a learning process, durations of all trials within one condition were averaged and compared across conditions with a 2-way ANOVA (see main section statistics).

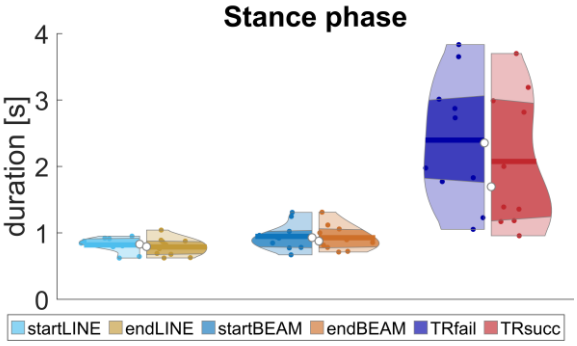

Figure 8: *Stance phase duration (in seconds [s]) of each condition. Violin plots: each colored circle represents one participant; thick lines represent mean values; white circles indicate median values; dark areas indicate quartiles.*

Results

A significant effect of TASK ($p < 0.001$), TIME ($p < 0.05$) and the interaction TASK × TIME ($p < 0.05$) was found on the duration of stance phases. TIGHTROPE had longer stance

phases ($p < 0.001$) than LINE and BEAM, with no difference between the latter two. Contrasts showed significantly shorter stance phases in TRsucc than TRfail ($p < 0.05$) (Figure 8).

EMG – trial specific low pass cutoff frequency

Methods

Reviews by Hug et al. (2011) and Turpin et al. (2021) call for greater awareness of the choice of cutoff frequencies for low-pass filters, prior to synergy extraction. Simply put, a lower cutoff frequency leads to a smoother EMG envelope. This 'wider' activation profile contains less variation and probably more overlap between different muscle profiles, which naturally affects synergy results. Several studies have investigated the effect of different low-pass filters on extracted motor modules. For instance, lower cutoff frequencies led to a higher total variance accounted for (tVAF) at a given number of synergies, which consequently also affected the choice of the required synergy number (NoS) for a movement (Hug, 2011; Hug et al., 2012; Kieliba et al., 2018; Shuman et al., 2017; van der Krogt et al., 2016). However, Hug et al. (2012) showed, that NoS was not affected by different cutoff frequencies, when the knee-point method was applied (as also used in the current study) in contrast to fixed thresholds (e.g. tVAF ≥ 90%). Moreover, low-pass filters also altered synergy vectors W and activation coefficients C extracted via NNMF (Kieliba et al., 2018; Shuman et al., 2017). This is not only a problem when various studies are compared, but also matters when movements with different duration times are investigated within the same study (Hug, 2011). To address this issue recent studies tried to gain similar smoothed electromyography (EMG) profiles by determining the low-pass cutoff frequency in relation to movement duration, e.g. 5 – 12 Hz for 60 – 140% of an optimal pedaling rate according to pedaling rates (Hug et al., 2011), 9 Hz for walking and 12 Hz for pedaling based on a machine learning pattern recognition algorithm (Hug et al., 2019), or by dividing a fixed cutoff frequency by the trial specific duration, i.e. 3.5 Hz/duration for treadmill walking (Meyer et al., 2016) and 7 Hz/duration for overground walking of post-stroke patients (Banks et al., 2017). For the current study, we used the same procedure as Banks et al. (2017) and determined a trial specific cutoff frequency for the low-pass filter - 7 Hz/trial-duration. All other EMG processing and synergy extraction steps were done the same way as our main analysis (main section). We aimed to determine whether the different durations would alter our main synergy results in terms of complexity, distinctness, and trial-to-trial variability. Figure 9 shows, how different cutoff frequencies affect EMG smoothing.

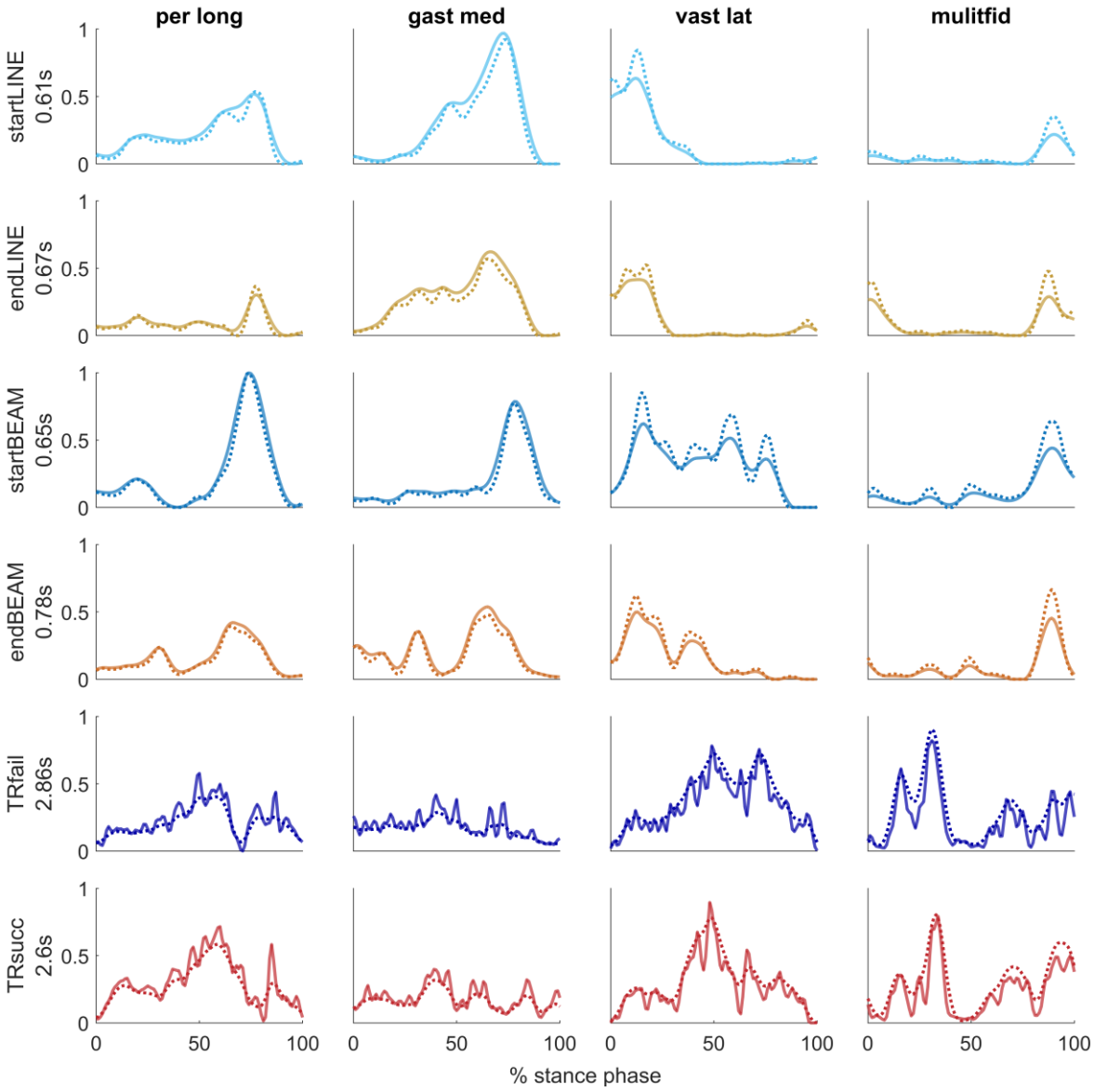

Figure 9: *Example of the influence of different cutoff frequencies on EMG smoothing of four muscles (one trial per condition, of one participant). The solid lines represent the fixed low-pass cutoff frequency (7 Hz), and the dashed lines represent the duration-dependent cutoff frequency (7 Hz/trial duration). The duration of the trials is shown on the y axis and given in seconds [s].*

Results

An average of 5.6 ± 2.22 NoS was determined among participants. For tVAF1 a significant effect of TASK ($p < 0.001$) was observed, with highest tVAF1 in TIGHTROPE, followed by BEAM and LINE at last ($p < 0.001$). There was also a significant effect of TASK in tVAFNoS ($p < 0.05$) which was higher in TIGHTROPE compared to LINE ($p < 0.05$). Regarding the distinctness of activation coefficients, the ANOVA revealed a significant effect of TASK for r ($p < 0.02$), r_{max} and %lag ($p < 0.001$). Activation coefficients were more correlated to each other (r: $p < 0.01$; r_{max}: $p < 0.001$) in TIGHTROPE compared to LINE and

BEAM. The lag% was higher in LINE than BEAM ($p < 0.05$) and lowest in TIGHTROPE ($p < 0.001$). Additionally, r_{max} was significantly affected by the interaction TASK × TIME ($p < 0.05$), where contrasts revealed a decrease during learning on the TIGHTROPE ($p < 0.05$) (Figure **10**).

Regarding trial-to-trial similarity, there was a significant effect of TASK ($p < 0.001$) on r, with highest correlations in LINE, followed by BEAM ($p < 0.01$) and TIGHTROPE at last ($p < 0.001$). Correlation was also significantly affected by TIME ($p < 0.05$), where contrasts revealed an increase during learning on the TIGHTROPE ($p < 0.05$). There were no significant differences in cross-correlations r_{max} and %lag (Figure 10, Figure 11).

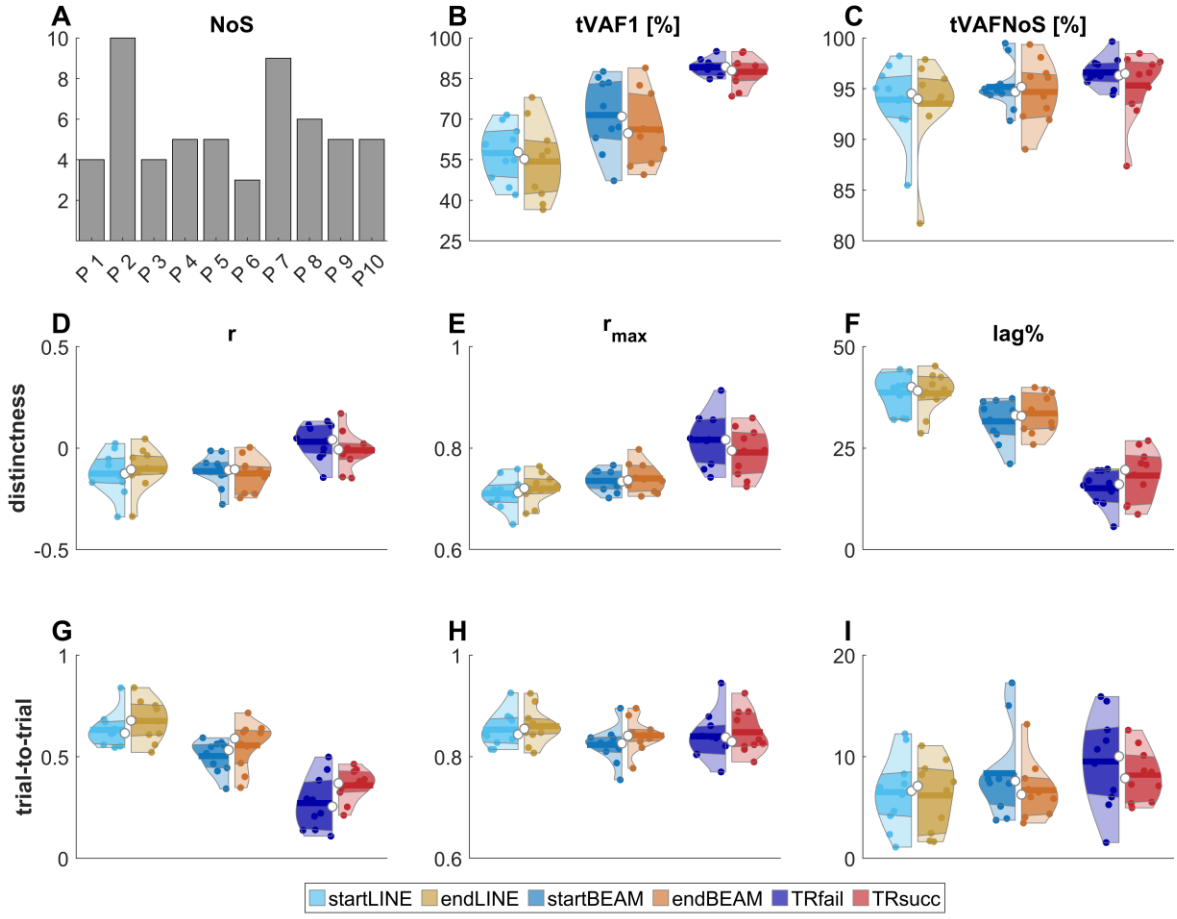

Figure 10: *Synergies were extracted of EMG signals filtered with the duration-dependent cutoff frequencies.* ***A:*** *bars show the number of required synergies (NoS) for each participant (P1 – P10).* ***B-C:*** *the total variance accounted for one synergy (****B:*** *tVAF1) and NoS (****C:*** *tVAFNoS).* ***D-F:*** *Synergy activation coefficient distinctness and* ***G-I:*** *trial-to-trial similarity measured by Pearson correlation (****D, G****: r), maximum cross-correlation coefficient (****E, H:*** *r_{max}) and lag at r_{max} (****F, I:*** *lag%). Violin plots: each colored circle represents one participant; thick lines represent mean values; white circles indicate median values; dark areas indicate quartiles.*

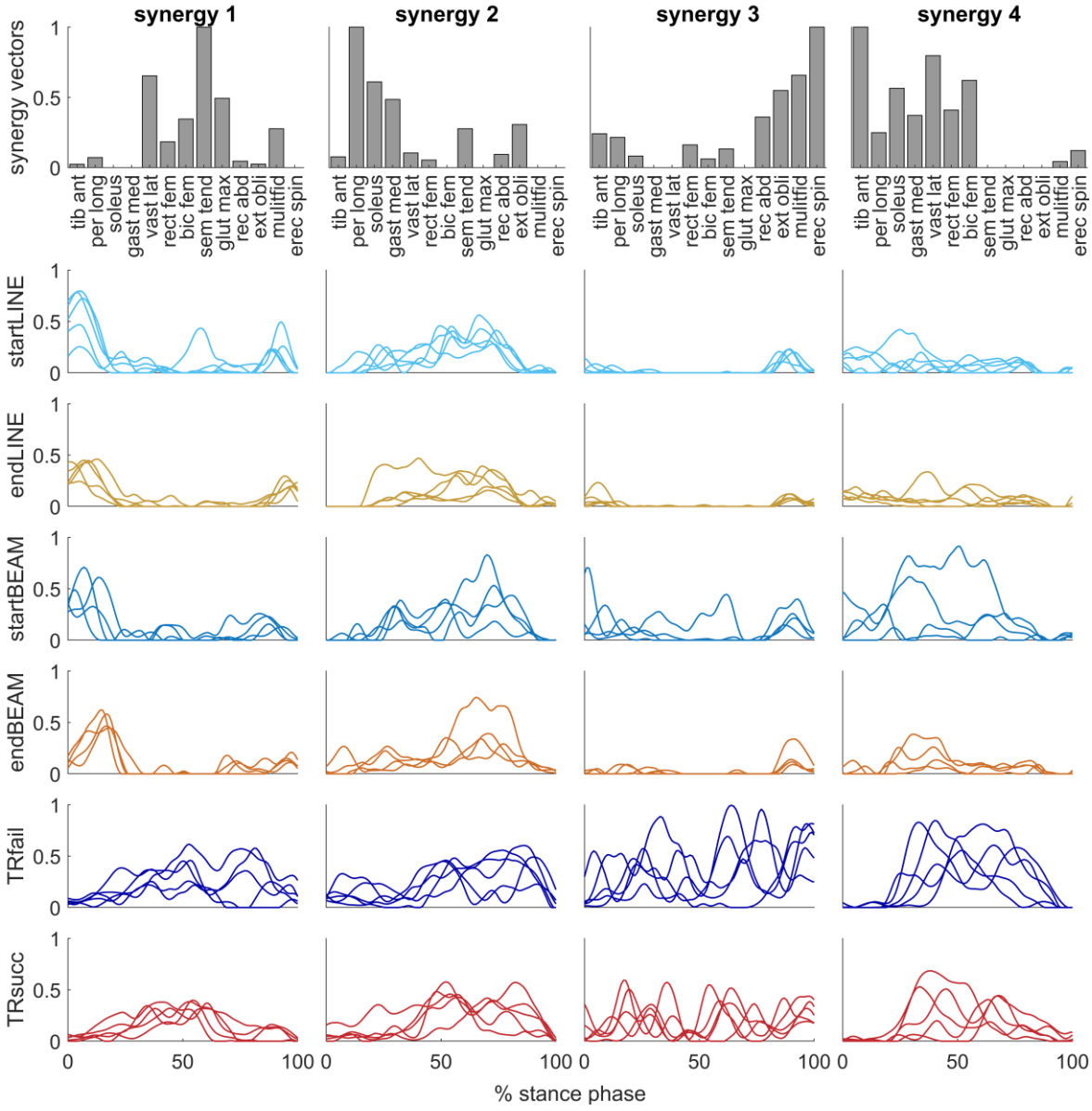

Figure 11: *All extracted synergy vectors (bar plots) and corresponding activation coefficients (waveform plots in the same column) for each condition of one participant (P3). Each waveform represents the activation coefficient of one trial.*

Muscle synergy extraction from each condition independently

Methods

To investigate whether similar motor modules were utilized across different walking conditions, we performed individual synergy extraction for each condition using the procedures described in the main paper. For this purpose, we concatenated the EMG matrices within each condition, and employed NNSVDLRC and NNMF. We performed two widely used analyses on this data. In the first step of our analysis, we compared synergy vectors across all possible pairs among conditions using the Pearson correlation coefficient (r). A

pair of synergy vectors was considered as similar (= shared), if r > 0.684, which corresponds to the critical value of r for 13 muscles at p = 0.01 (Allen et al., 2020; Allen et al., 2019; Allen et al., 2017; Chvatal et al., 2011; Frère & Hug, 2012; Safavynia & Ting, 2012; Zhao et al., 2021). To account for variations in the number of synergies (NoS) across conditions and participants, we visualized the number of shared synergies (n_{shared}) as percentage. The percentage of shared synergies ($\%n_{shared}$) was calculated using equation (3), where subscripts *condition1* and *condition2* indicate the two compared conditions (e.g., startLINE and endLINE).

$$(3) \quad \%n_{shared} = 100 \frac{n_{shared}}{min\ (NoS_{condition1},\ NoS_{condition2})}$$

In the second step, we reconstructed synergy activation coefficients for all conditions using the synergy vectors (W) from either startLINE or startBEAM. We employed a commonly used reconstruction algorithm (Boccia et al., 2018; Frère & Hug, 2012; Gizzi et al., 2011; Hug et al., 2011; Kristiansen et al., 2016; Muceli et al., 2010; van den Hoorn et al., 2015) based on the updating rule for NNMF proposed by Lee and Seung (2001), as described in equations (4). W from one condition was held fixed (suffix: fix) to reconstruct C (suffix: rec), with the corresponding EMG matrix (E) from another condition. After an initial random guess for the reconstruction matrix, numerous iterations (n, here ranging from 50 to 5000) were made until the function f(W,C) reached a convergence criterion (10^{-5}) described in equation (5). Subscripts i and j indicate the row and column, while superscript T indicates the transposed matrix. Crec was used to calculate the reconstructed tVAF (tVAFrec), together with E and Wfix. Consistent with previous studies (Boccia et al., 2018; Heales et al., 2016; Oliveira et al., 2016), synergy vectors were assumed to be similar across conditions if the tVAFrec exceeded 80%.

$$(4) \quad Crec_{ij}^{(n)} = Crec_{ij}^{(n-1)} \left(\frac{(Wfix^T\ E)_{ij}}{(Wfix^T\ Wfix\ Crec^{(n-1)})_{ij}} \right);$$

$$(5) \quad f(Wfix, Crec) = \frac{\|E - Wfix\ Crec\|_F}{\sqrt{m\ n}}$$

Results

Figure 12 shows the high amount of shared synergy vectors across the LINE and BEAM tasks for all participants. A high range, and on average a smaller $\%n_{shared}$ was found between LINE or BEAM conditions with TIGHTROPE conditions across participants. Reconstruction procedures revealed, that tVAFrec was > 80% in all participants, for all LINE

and BEAM conditions. In contrast, only six participants exceeded the threshold in TIGHTROPE conditions, if activation coefficients were reconstructed by synergy vectors of startLINE. If activation coefficients were reconstructed by startBEAM, tVAFrec of one participant was under our criterium for TRfail and two participants for TRsucc (Figure 12).

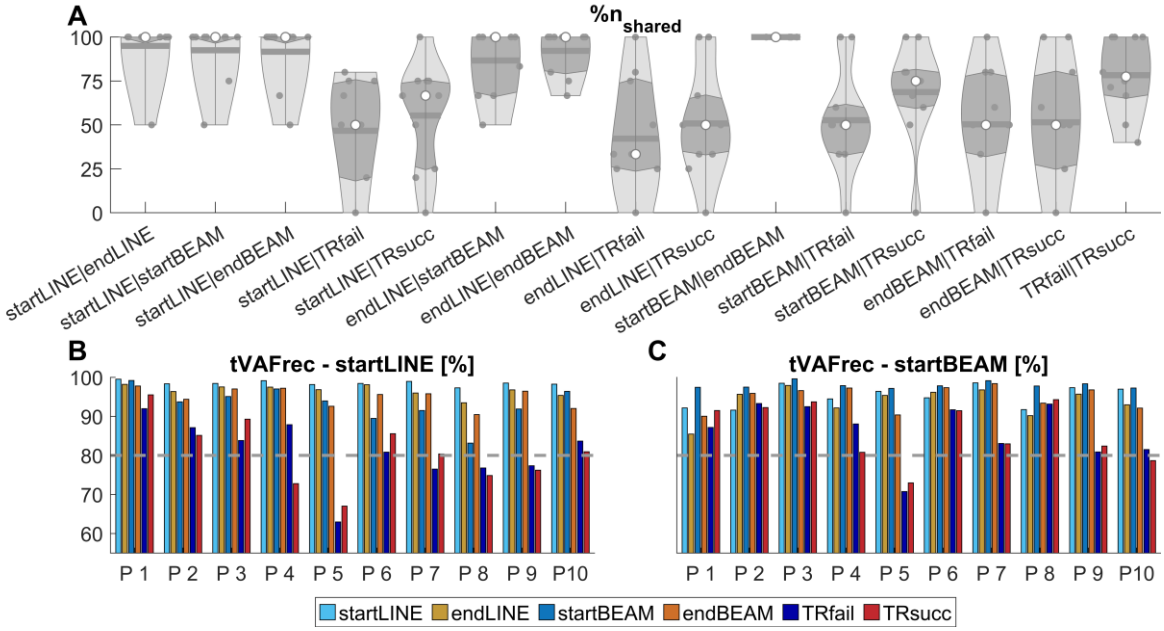

Figure 12: ***A:*** *The percentage of shared synergy vectors ($n\%_{shared}$) for all possible pairs of condition comparisons.* ***B-C:*** *the tVAF of reconstructed activation coefficients (tVAFrec) of the synergy vectors of either startLINE (**B**) or startBEAM (**C**) for all participants (P) and conditions. Violin plots: each grey circle represents one participant; thick lines represent mean values; white circles indicate median values; dark areas indicate quartiles.*

Discussion

Here we want to deeper discuss our approach on extracting synergies over different conditions. Similar tVAFNoS values (main section) indicate, that extracted synergies reflect EMG variability equally among conditions. However, computing muscle synergies over different conditions has previously been done only in few studies (Chvatal & Ting, 2013; Hagio et al., 2015; Hug et al., 2011; Roh et al., 2012; Safavynia & Ting, 2012). We here utilized this approach due to the following four considerations: (1) similar movement goals are controlled via similar muscle synergies, (2) the small number of trials within each condition, (3) computing trial-to-trial similarity among similar synergy vectors, and (4) the computational problem of extracting accurate synergies, if activation coefficients timing overlaps.

(1) As outlined in the introduction, an important feature of motor control is the recruitment of similar synergy vectors for similar mechanical goals across various tasks (Allen et al., 2020; Barroso et al., 2014; Chvatal et al., 2011; Hug et al., 2011; Nazifi et al., 2017; Oliveira et al., 2016). In the current study, the same movement goal – performing a step – was intended in all conditions. Therefore, we hypothesized that similar synergy vectors were used. In an additional analysis, synergies were extracted from each condition independently (Chvatal & Ting, 2013; Hagio et al., 2015; Hug et al., 2011) to verify this assumption. In a first step, we analyzed the percentage of shared synergy vectors ($r > 0.684$ (Allen et al., 2020; Allen et al., 2019; Allen et al., 2017; Chvatal et al., 2011; Frère & Hug, 2012; Safavynia & Ting, 2012; Zhao et al., 2021)). While a high percentage of vectors was shared among LINE and BEAM conditions, less synergies were shared if LINE and BEAM conditions were compared to TRfail or TRsucc (Figure 12). In a second step, we reconstructed the activation coefficients of all conditions with synergy vectors of startLINE or startBEAM. We found sufficient reconstruction performance (tVAF > 80% (Boccia et al., 2018; Heales et al., 2016; Oliveira et al., 2016)) for all LINE and BEAM conditions (Figure 12). When reconstructing TIGHTROPE conditions from startLINE, 6 participants achieved a tVAF above 80%, while for startBEAM, it was achieved by 9 participants in TRfail and 8 participants in TRsucc. Turpin et al. (2017) found that some synergies were barely activated in cycling with low exercise intensity, which could lead to poor performances of factorization methods in detecting them (Tresch et al., 2006; Turpin et al., 2021). Similarly, in our study, we observed differences in the contribution of synergy vectors across conditions (Figure 5). Cluster 2, primarily composed of trunk muscles, had a tVAF below 10% for LINE and BEAM conditions but exceeded the threshold for TIGHTROPE. This may explain the relatively lower reconstruction accuracy of TIGHTROPE compared to LINE and BEAM conditions since these synergies were probably not captured by extracting synergies separately. Furthermore, cluster 1, predominantly composed of quadriceps and gluteus muscles, exhibited a tVAF below 10% in most LINE synergies but only in some BEAM synergies, which could explain higher reconstruction accuracies of TIGHTROPE when using startBEAM rather than startLINE. The reconstruction results, combined with cluster analyses, indicate that there is a presence of similar synergy vectors across tasks, but additional synergies are either added or more activated during balancing tasks. The low percentage of shared synergies in some participants may be due to the difficulty of accurately extracting synergy vectors when their activation timing overlaps (see below).

(2) Several studies proposed the importance of variability in EMG data by concatenated trials for synergy computation (Oliveira et al., 2014; Ranganathan & Krishnan, 2012; Steele, Tresch, et al., 2015; Turpin et al., 2021). Oliveira et al. (2014) suggested to compute muscle synergies over a minimum of 20 concatenated gait-cycles. Due to the within-session design of the current study, each condition only included four to five stance-phases. Concatenating data of all conditions resulted in a total of 24 to 30 stance phases per participants.

(3) To ensure that the variability of activation coefficients could be meaningful quantified, the same synergy vectors were used across conditions. This is in line with Cheung et al. (2020) who first clustered synergy vectors among bowling sessions and reconstructed EMG matrices of each session with the cluster centroids.

(4) Increasing the time overlap (= correlation) of synergy activation coefficients in simulated or real datasets, decreases the accuracy of extracted synergy vectors. Namely, with sufficient coupling, synergy vectors merged, due to underlying assumptions of factorization algorithms (Soomro et al., 2018; Steele, Tresch, et al., 2015; Tresch et al., 2006). In our opinion, the distinctness and timing of activation coefficients might reflect an essential feature for movement proficiency and learning. Calculating muscle synergies over all conditions may overcome limitations of extracting algorithms.

With this additional analysis we showed that similar synergies were utilized through the tasks. Moreover, we hypothesize that calculating synergies over different tasks with similar movement goals (i.e.: performing a step), provides salient information in synergy analysis.

Results of individual muscles and joints

Muscle activations individual

Trial-to-trial similarity in muscle activation patterns measured by Pearson correlation coefficient (r) was significantly affected by TASK in all muscles apart from rec_abd and ext_obli (tib_ant, per_long: $p < 0.05$; rect_fem: $p < 0.01$; others: $p < 0.001$). Trial-to-trial similarity was smaller for TIGHTROPE than BEAM in eight muscles (vast_lat: $p < 0.05$; soleus, gast_med, bic_fem, sem_tend, glut_max, multifid, erec_spin: $p < 0.001$), and smaller for TIGHTROPE compared with LINE in all muscles (tib_ant, per_long: $p < 0.05$; rect_fem: $p < 0.01$; others: $p < 0.001$). Trial-to-trial similarity was smaller for BEAM compared to LINE in five muscles (soleus, rect_fem: $p < 0.05$; multifid: $p < 0.01$; gast_med, erec_spin: $p < 0.001$). Additionally, similarity was significantly affected by TIME (per_long, gast_med, glut_max: $p < 0.05$), and TASK × TIME (gast_med, glut_max: $p < 0.05$; soleus: $p < 0.01$) in three muscles. Contrasts revealed higher similarities in endBEAM than startBEAM (gast_med, multifid: $p < 0.05$, erec_spin: $p < 0.01$) and TRsucc than TRfail (per_long, gast_med, glut_max: $p < 0.05$) (Table 2).

Table 2: *Mean (M) and standard deviation (SD) among participants of for trial-to-trial similarity measured by Pearson correlation coefficient r for all conditions and muscles. ANOVA revealed significant effects of TASK in all muscles apart from rec_abd and ext_obli. Significant differences observed by contrasts are indicated by *.*

	LINE				**BEAM**				**TIGHTROPE**			
	start		**end**		**start**		**end**		**fail**		**succ**	
	M	*SD*	*M*	*SD*	*M*	*SD*	*M*	*SD*	*M*	*SD*	*M*	*SD*
tib_ant	0.49	0.22	0.60	0.17	0.43	0.15	0.45	0.20	0.36	0.19	0.36	0.21
per_long	0.49	0.22	0.61	0.20	0.45	0.16	0.48	0.22	0.31*	0.16	0.44*	0.19
soleus	0.84	0.07	0.80	0.10	0.64	0.18	0.67	0.17	0.23	0.19	0.31	0.18
gast_med	0.83	0.08	0.83	0.08	0.61*	0.21	0.69*	0.19	0.17*	0.16	0.31*	0.11
vast_lat	0.78	0.20	0.73	0.28	0.56	0.23	0.60	0.20	0.31	0.18	0.41	0.16
rect_fem	0.62	0.23	0.63	0.31	0.36	0.28	0.47	0.33	0.24	0.13	0.36	0.18
bic_fem	0.66	0.20	0.70	0.18	0.55	0.29	0.60	0.16	0.27	0.17	0.31	0.11
sem_tend	0.63	0.27	0.76	0.17	0.62	0.24	0.65	0.18	0.23	0.14	0.26	0.16
glut_max	0.81	0.08	0.79	0.18	0.61	0.23	0.70	0.20	0.14*	0.18	0.32*	0.12
rec_abd	0.15	0.23	0.02	0.12	0.13	0.20	0.08	0.09	0.11	0.07	0.11	0.14
ext_obli	0.28	0.18	0.26	0.23	0.16	0.21	0.29	0.16	0.07	0.11	0.18	0.18
multifid	0.82	0.09	0.85	0.06	0.57*	0.25	0.68*	0.16	0.10	0.10	0.17	0.18
erec_spin	0.62	0.14	0.69	0.18	0.35*	0.21	0.49*	0.20	0.10	0.08	0.11	0.10

Trial-to-trial similarity measured by cross-correlation coefficient (r_{max}) was significantly affected by TASK in six muscles (soleus, gast_med, glut_max, ext_obli, multifid, erec_spin: $p < 0.001$), where TIGHTROPE similarity was smaller than BEAM (soleus: $p < 0.05$; others: $p < 0.001$) and LINE ($p < 0.001$). BEAM similarity was smaller than LINE in four muscles (soleus: $p < 0.05$; gast_med, multifid, erec_spin: $p < 0.001$). Additionally, similarity was also significantly affected by TIME in four muscles (per_long, soleus, gast_med, multifid, erec_spin: $p < 0.05$) with higher similarities in END, and TASK × TIME in soleus ($p < 0.05$). Contrasts revealed higher similarities in endLINE than startLINE (erec_spin: $p < 0.05$), endBEAM than startBEAM (soleus, gast_med, erec_spin: $p < 0.05$) and TRsucc than TRfail (multifid: $p < 0.05$; soleus: $p < 0.01$) (

Table 3).

Table 3: *Mean (M) and standard deviation (SD) among participants of for trial-to-trial similarity measured by the maximum cross-correlation coefficient r_{max} for all conditions and muscles. ANOVA revealed significant effects of TASK in soleus, gast_med, glut_max, ext_obli, multifid and erec_spin. Significant differences observed by contrasts are indicated by *.*

	LINE				**BEAM**				**TIGHTROPE**			
	start		**end**		**start**		**end**		**fail**		**succ**	
	M	*SD*	*M*	*SD*	*M*	*SD*	*M*	*SD*	*M*	*SD*	*M*	*SD*
tib_ant	0.81	0.06	0.83	0.06	0.85	0.04	0.86	0.04	0.87	0.04	0.87	0.07
per_long	0.88	0.05	0.90	0.04	0.87	0.05	0.87	0.06	0.88	0.02	0.90	0.03
soleus	0.96	0.02	0.95	0.02	0.91*	0.04	0.93*	0.03	0.87*	0.04	0.90*	0.03
gast_med	0.95	0.03	0.95	0.03	0.88*	0.04	0.92*	0.04	0.84	0.03	0.86	0.04
vast_lat	0.91	0.05	0.89	0.08	0.85	0.08	0.87	0.06	0.86	0.05	0.86	0.06
rect_fem	0.85	0.09	0.85	0.08	0.80	0.07	0.84	0.09	0.82	0.06	0.84	0.06
bic_fem	0.83	0.06	0.84	0.07	0.84	0.05	0.83	0.05	0.82	0.04	0.80	0.04
sem_tend	0.86	0.07	0.89	0.05	0.85	0.08	0.86	0.03	0.83	0.05	0.80	0.07
glut_max	0.92	0.04	0.92	0.04	0.88	0.06	0.90	0.05	0.77	0.06	0.79	0.08
rec_abd	0.72	0.07	0.72	0.06	0.74	0.07	0.72	0.05	0.69	0.04	0.71	0.08
ext_obli	0.82	0.04	0.82	0.04	0.81	0.05	0.82	0.03	0.72	0.05	0.76	0.05
multifid	0.90	0.05	0.92	0.03	0.83	0.07	0.86	0.05	0.72*	0.06	0.76*	0.07
erec_spin	0.83*	0.05	0.89*	0.07	0.76*	0.08	0.80*	0.07	0.67	0.03	0.68	0.07

The lag% was significantly affected by TASK for all muscles apart from multifid and erec_spin (tib_ant, per_long, soleus, rec_abd: $p < 0.05$: gast_med; rect_fem, bic_fem, multifid: $p < 0.01$; others: $p < 0.001$). lag% was significantly lower in TIGHTROPE than BEAM for per_long (per_long: $p < 0.05$). For all other muscles TIGHTROPE had a higher lag% than LINE (tib_ant, gast_med, rec_abd: $p < 0.05$; soleus, rect_fem, bic_fem, multifid: $p < 0.01$; others: $p < 0.001$) and for sem_tend and glut_max also than BEAM ($p < 0.001$). BEAM had higher lag% than LINE in three muscles (gast_med, bic_fem: $p < 0.05$; vast_lat: $p < 0.01$) (

Table **4**).

Table 4: *Mean (M) and standard deviation (SD) among participants of for trial-to-trial similarity measured by the lag time lag% at the maximum cross-correlation coefficient for all conditions and muscles. ANOVA revealed significant effects of TASK in all muscles apart from multifid and erec_spin.*

	LINE				**BEAM**				**TIGHTROPE**			
	start		**end**		**start**		**end**		**fail**		**succ**	
	M	*SD*	*M*	*SD*	*M*	*SD*	*M*	*SD*	*M*	*SD*	*M*	*SD*
tib_ant	6.06	7.58	5.55	5.02	5.60	4.01	6.64	4.88	9.26	5.93	10.24	7.67
per_long	6.84	3.79	5.54	4.41	7.62	3.88	7.06	3.44	5.13	3.06	3.82	2.20
soleus	1.98	0.63	2.95	1.46	4.58	1.11	3.66	2.13	6.95	4.92	6.09	3.09
gast_med	2.94	1.18	2.72	0.81	5.63	2.33	4.39	1.76	6.68	4.49	6.56	3.79
vast_lat	2.89	3.32	3.39	7.39	7.09	7.59	5.04	3.76	6.93	2.86	7.99	4.22
rect_fem	3.30	3.89	6.44	11.24	7.06	7.24	9.08	11.58	10.93	3.64	8.76	4.60
bic_fem	7.43	9.48	5.74	10.69	5.51	6.17	5.98	5.98	6.60	3.78	12.33	5.80
sem_tend	3.92	5.89	3.10	5.58	5.23	8.82	1.63	1.83	8.37	5.12	9.17	5.52
glut_max	2.16	1.10	3.19	3.85	5.20	4.17	5.33	6.02	13.76	4.57	11.47	7.26
rec_abd	17.52	8.52	20.07	5.64	16.26	8.22	17.80	8.88	11.81	3.78	12.80	6.11
ext_obli	8.43	6.32	8.07	5.82	7.45	3.80	8.62	5.34	8.63	5.16	9.14	6.11
multifid	0.90	0.61	3.78	6.61	4.95	5.35	4.32	7.74	6.98	4.70	6.22	6.70
erec_spin	7.94	8.33	10.15	14.38	15.95	12.86	14.14	17.25	11.02	7.92	12.78	8.24

Joint abbreviations

Joints: ankle plantar-/dorsiflexion (ankle), knee flexion/extension (knee), hip flexion/extension (hip_f), hip ab-/adduction (hip_a), hip internal/external rotation (hip_r), lumbar flexion/extension (lum_f), lumbar medial/lateral bending (lum_b), and lumbar internal/external rotation (lum_r).

Joint angles individual

Trial-to-trial similarity measured by Pearson correlation coefficient (r) was significantly affected in all joints by TASK (ankle: $p < 0.01$; others: $p < 0.001$). TIGHTROPE similarity was always lower than BEAM (ankle; $p < 0.05$; others: $p < 0.001$) and LINE (ankle: $p < 0.01$; others: $p < 0.001$). BEAM similarity was lower than LINE in three joints (knee, hip_a: $p < 0.05$; lum_b: $p < 0.001$). It was also significantly affected by TIME in some joints (hip_a, hip_r, lum_r: $p < 0.05$; ankle, hip_f: $p < 0.01$), with lower similarity in START than END. Additionally, a significant effect of TIME × TASK was found in two joints (hip_r: $p < 0.01$; hip_f: $p < 0.001$). Contrasts showed that r was lower in startLINE than endLINE (hip_a: $p < 0.05$) and TRfail than TRsucc (ankle: $p < 0.05$) (Table 5).

Table 5: *Mean (M) and standard deviation (SD) among participants of for trial-to-trial similarity measured by Pearson correlation coefficient r for all conditions and joint angles. ANOVA revealed significant effects of TASK in all joints Significant differences observed by contrasts are indicated by *.*

	LINE				**BEAM**				**TIGHTROPE**			
	start		**end**		**start**		**end**		**fail**		**succ**	
	M	*SD*	*M*	*SD*	*M*	*SD*	*M*	*SD*	*M*	*SD*	*M*	*SD*
ankle	0.95	0.04	0.97	0.02	0.92	0.07	0.94	0.06	0.77*	0.21	0.88*	0.06
knee	0.97	0.02	0.97	0.02	0.93	0.07	0.91	0.07	0.53	0.31	0.54	0.27
hip_f	0.96	0.10	0.99	0.01	0.95	0.14	0.97	0.04	0.66	0.32	0.88	0.12
hip_ab	0.89*	0.15	0.96*	0.02	0.69	0.35	0.76	0.28	0.19	0.20	0.31	0.20
hip_r	0.94	0.13	0.97	0.01	0.90	0.20	0.96	0.05	0.55	0.36	0.76	0.17
lum_f	0.71	0.18	0.69	0.24	0.46	0.28	0.56	0.31	0.01	0.17	0.22	0.28
lum_b	0.88	0.16	0.90	0.15	0.40	0.33	0.56	0.32	0.08	0.18	-0.04	0.21
lum_r	0.93	0.14	0.98	0.02	0.82	0.26	0.88	0.26	0.31	0.29	0.38	0.38

Trial-to-trial similarity measured by cross-correlation coefficient (r_{max}) was significantly affected by TASK in all joints (lum_f: $p < 0.05$; hip_f, hip_r: $p < 0.05$; others: $p < 0.001$). TIGHTROPE similarity was lower than BEAM in six joints (ankle, lum_f, lum_b: $p < 0.05$; knee, hip_a, lum_r: $p < 0.001$) and LINE in all joints (hip_f, hip_r: $p < 0.05$; lum_f: $p < 0.01$; othert: $p < 0.001$). BEAM similarity was lower than LINE in lum_b ($p < 0.01$). It was also significantly affected by TIME in two joints (lum_r: $p < 0.01$; lum_f: $p < 0.001$), with lower similarity in START than END. Additionally, a significant effect of TIME × TASK was found in lum_r ($p < 0.05$). Contrasts showed that r_{max} was lower in startBEAM than endBEAM (lum_f, lum_b: $p < 0.05$) and TRfail than TRsucc (lum_f: $p < 0.01$) (Table 6).

Table 6: *Mean (M) and standard deviation (SD) among participants of for trial-to-trial similarity measured by the maximum cross-correlation coefficient r_{max} for all conditions and joint angles. ANOVA revealed significant effects of TASK in all joints Significant differences observed by contrasts are indicated by *.*

	LINE				**BEAM**				**TIGHTROPE**			
	start		**end**		**start**		**end**		**fail**		**succ**	
	M	*SD*	*M*	*SD*	*M*	*SD*	*M*	*SD*	*M*	*SD*	*M*	*SD*
ankle	0.94	0.05	0.97	0.01	0.89	0.11	0.93	0.05	0.73	0.18	0.81	0.15
knee	0.97	0.06	0.98	0.01	0.96	0.08	0.97	0.04	0.95	0.04	0.96	0.03
hip_f	0.96	0.08	0.99	0.01	0.94	0.13	0.97	0.03	0.95	0.03	0.96	0.03
hip_ab	0.97	0.03	0.99	0.01	0.92	0.07	0.90	0.13	0.56	0.19	0.66	0.14
hip_r	0.90	0.13	0.96	0.04	0.87	0.14	0.93	0.04	0.78	0.19	0.86	0.17
lum_f	0.83	0.20	0.90	0.17	0.79*	0.19	0.91*	0.14	0.61*	0.17	0.80*	0.16
lum_b	0.85	0.08	0.88	0.15	0.65*	0.18	0.68*	0.19	0.49	0.09	0.49	0.13
lum_r	0.92	0.07	0.95	0.03	0.82	0.16	0.88	0.15	0.50	0.20	0.65	0.21

The lag% was significantly affected by TASK in five joints (hip_r, lum_f: $p < 0.01$; hip_a, lum_b, lum_r: $p < 0.001$). TIGHTROPE had a higher lag% than BEAM in four joints (hip_a, hip_r, lum_r: $p < 0.01$; lum_b: $p < 0.001$) and LINE in all five joints (hip_r, lum_r: $p < 0.01$; other: $p < 0.001$). BEAM had a higher lag% than LINE in two jonts (hip_a: $p < 0.05$; lum_b: $p < 0.001$). There was a significant effect of TIME in five joints (hip_a, lum_f, lum_r: $p < 0.01$; knee, hip_r: $p < 0.001$) with higher lag% in START. Additionally, there was a significant effect of TASK × TIME in three joints (knee, hip_a: $p < 0.01$; hip_r: $p < 0.001$). Contrasts revealed higher lag% in startLINE than endLINE in hip_a ($p < 0.05$). For lum_f, startBEAM and TRfail had significantly higher lag% compared to endBEAM and TRsucc ($p < 0.01$), respectively (Table 7).

Table 7: *Mean (M) and standard deviation (SD) among participants of for trial-to-trial similarity measured by the lag time lag% at the maximum cross-correlation coefficient for all conditions and joint angles. ANOVA revealed significant effects of TASK in hip_r, hip_a, lum_b, lum_f. Significant differences observed by contrasts are indicated by *.*

	LINE				**BEAM**				**TIGHTROPE**			
	start		**end**		**start**		**end**		**fail**		**succ**	
	M	*SD*	*M*	*SD*	*M*	*SD*	*M*	*SD*	*M*	*SD*	*M*	*SD*
ankle	0.22	0.44	0.00	0.00	4.35	12.2	1.04	2.85	8.75	18.91	3.18	8.21
knee	0.00	0.00	0.00	0.00	0.00	0.00	0.00	0.00	0.03	0.09	0.00	0.00
hip_f	2.76	8.73	0.00	0.00	2.00	6.32	0.00	0.00	0.89	1.86	0.23	0.74
hip_a	2.42*	4.79	0.55*	0.56	7.51	9.51	7.75	11.83	32.02	15.47	21.63	10.85
hip_r	3.82	9.94	0.22	0.40	4.68	12.77	0.86	1.17	13.14	13.23	3.30	8.99
lum_f	10.92	15.24	4.03	10.93	17.89*	17.68	4.44*	11.05	24.66*	16.25	11.48*	11.94
lum_b	2.62	5.32	5.71	14.86	19.90	14.77	19.23	17.12	40.14	8.57	44.70	12.60
lum_r	2.55	6.77	0.49	1.05	8.85	13.36	4.74	11.61	31.68	18.03	18.96	14.74

Eidesstattliche Erklärung

Ich, Paul Kaufmann, erkläre, dass ich die vorliegende Arbeit selbstständig verfasst habe und nur die ausgewiesenen Hilfsmittel verwendet habe. Diese Arbeit wurde weder an einer anderen Stelle eingereicht (z. B. für andere Lehrveranstaltungen) noch von anderen Personen (z. B. Arbeiten von anderen Personen aus dem Internet) vorgelegt.

Schützen am Gebirge, am 03.07.2023